1101

NATIONAL ADVISORY COMMITTEE FOR AERONAUTICS

TECHNICAL NOTE

No. 1101

TANK TESTS TO DETERMINE THE EFFECT OF VARYING DESIGN PARAMETERS OF PLANING-TAIL HULLS

II - EFFECT OF VARYING DEPTH OF STEP, ANGLE OF AFTERBODY KEEL, LENGTH OF AFTERBODY CHINE, AND GROSS LOAD

By John R. Dawson, Robert McKann, and Elizabeth S. Hay

Langley Memorial Aeronautical Laboratory
Langley Field, Va.

Washington
July 1946

NATIONAL ADVISORY COMMITTEE FOR AERONAUTICS

TECHNICAL NOTE NO. 1101

TANK TESTS TO DETERMINE THE EFFECT OF VARYING DESIGN PARAMETERS OF PLANING-TAIL HULLS

II - EFFECT OF VARYING DEPTH OF STEP, ANGLE OF AFTERBODY KEEL, LENGTH OF AFTERBODY CHINE, AND GROSS LOAD

By John R. Dawson, Robert McKann, and Elizabeth S. Hay

SUMMARY

The second part of a series of tests made in Langley tank no. 2 to determine the effect of varying design parameters of planing-tail hulls is presented. Results are given to show the effects on resistance characteristics of varying angle of afterbody keel, depth of step, and length of afterbody chine. The effect of varying the gross load is shown for one configuration. The resistance characteristics of planing-tail hulls are compared with those of a conventional flying-boat hull. The forces on the forebody and afterbody of one configuration are compared with the forces on a conventional hull.

Increasing the angle of afterbody keel had small effect on hump resistance and no effect on high-speed resistance but increased free-to-trim resistance at intermediate speeds.

Increasing the depth of step increased hump resistance, had little effect on high-speed resistance, and increased free-to-trim resistance at intermediate speeds.

Omitting the chines on the forward 25 percent of the afterbody had no appreciable effect on resistance. Omitting 70 percent of the chine length had almost no effect on maximum resistance but broadened the hump and increased spray around the afterbody.

Load-resistance ratio at the hump decreased more rapidly with increasing load coefficient for the planing-tail hull than for the representative conventional hull, although the load-resistance ratio at the hump was greater for the planing-tail hull than for the conventional hull throughout the range of loads tested. At speeds higher than hump speed, load-resistance ratio for the planing-tail hull was a maximum at a particular gross load and was slightly less at heavier and lighter gross loads.

The planing-tail hull was found to have lower resistance than the conventional hull at both the hump and at high speeds, but at intermediate speeds there was little difference. The lower hump resistance of the planing-tail hull was attributed to the ability of the afterbody to carry a greater percentage of the total load while maintaining a higher value of load-resistance ratio.

INTRODUCTION

In reference 1 are reported the results of preliminary tests made with models of an unconventional flying-boat hull called a planing-tail hull. The NACA planing-tail hull consists of a forebody having a pointed step of great depth leading into a very long afterbody. This afterbody extends back to the region where the tail surfaces would be attached; thus no tail extension is required behind the afterbody. The results of reference 1 indicated that this type hull might have some advantages over the hull of a conventional flying boat. This work was followed by a series of tests made to determine the effects on resistance characteristics of varying design parameters. Part I determined the effect of varying length, width, and plan-form taper of the afterbody. (See reference 2.) The present paper, part II, gives the results of tests made in Langley tank no. 2 to determine the effect of varying angle of afterbody keel, depth of step, length of afterbody chine, and gross load.

COEFFICIENTS AND SYMBOLS

The data of the tests were reduced to the following nondimensional coefficients based on Froude's criterion for similarity:

C_Δ load coefficient $\left(\frac{\Delta}{wb^3}\right)$

C_{Δ_o} gross load coefficient $\left(\frac{\Delta_o}{wb^3}\right)$

C_R resistance coefficient $\left(\frac{R}{wb^3}\right)$

C_V speed coefficient $\left(\frac{V}{\sqrt{gb}}\right)$

C_M trimming-moment coefficient $\left(\frac{M}{wb^4}\right)$

C_d draft coefficient $\left(\frac{d}{b}\right)$

where

Δ load on water, pounds

Δ_o gross load on water, pounds

R resistance, pounds

w specific weight of water (63.0 lb/cu ft in these tests)

b maximum beam of hull (1.08 ft)

V speed, feet per second

M trimming moment, pound-feet; moments tending to raise bow are considered positive

g acceleration of gravity, feet per second per second

d draft at step, feet

Other symbols used are

α angle of afterbody keel, degrees

x longitudinal distance from center of moments to step, inches; distance aft of step considered negative

H depth of step, inches

A part of afterbody over which chines are omitted, inches

B part of afterbody over which chines are retained, inches

σ sternpost angle, degrees

Δ/R load-resistance ratio

L_f/b forebody length-beam ratio

DESCRIPTION OF MODELS

In order to avoid effects of secondary variables not under study, the models were made with afterbodies that were very simple in form. Fillets and fairings were omitted; consequently the models would require further refinements before being made into hulls of good aerodynamic form.

The general lines of the models are given in figure 1 and table I lists the pertinent dimensions and parameters of each model. The forebody for all models is that of NACA model 35-A, which is the same forebody as was used in the tests reported in reference 3 and in the planing-tail-hull tests of reference 2; offsets of this forebody are given in reference 3.

The afterbody used in the tests to study angle of afterbody keel and depth of step was a prismatic form, pentagonal in section except for cylindrical sections from stations 12 to $13\frac{1}{2}$. Between these stations the afterbody was made cylindrical so that continuity could be maintained when parts of the chines were removed. The cylindrical sections cleared the water just below hump speed and remained clear at all higher speeds. The chines were omitted from parts of the afterbody by inserting lengths that were circular in section. The discontinuities between the circular and pentagonal sections were faired with plasticine. Although the model produced by this simple method was relatively crude, it should be adequate to show the effects of omitting chines on part of the afterbody.

The variations of the models tested are given in the following table:

Langley tank model	Depth of step	Angle of afterbody keel (deg)	Length of chine in percentage of length of afterbody
163A-1	0.35b	0	88.5
163A-6	.35b	2	88.5
163A-11	.35b	4	88.5
163A-16	.35b	6	88.5
163A-3	.50b	0	88.5
163A-13	.50b	4	88.5
163A-11A	.35b	4	75.0
163A-11B	.35b	4	30.0

TEST PROCEDURE

The tests were made by the specific method. All configurations were tested at a gross load coefficient of 1.00 and one model was tested also at gross load coefficients of 0.75 and 1.25. In order to simplify the tests, wing lift was assumed to vary only as the square of the speed, and the parabolic load curves of figure 2 were used. Fixed-trim runs at constant speeds were made and resistance, draft, and trimming moments were measured for each run. Sufficient trims were covered in the tests to give trim for minimum resistance, zero trimming moments for the center of moments used (fig. 1), and enough data to derive free-to-trim curves for a center of moments that would give zero trimming moment for best trim at the point of maximum resistance.

Resistance, as plotted, includes the air drag and the hydrodynamic resistance of the model since only the air drag of the towing gear was subtracted as a tare from the measured values of resistance. Trim, as measured, is the angle between the horizontal and the straight part of the forebody keel. Draft was measured vertically from the point of the step at the keel to the free-water surface.

At high speeds and low trims the afterbodies of the models were clear of all water and spray. Under these conditions, the resistance of the complete model can differ from that of the forebody alone by only the small

differences in air drag. Data from unpublished tests made with the forebody alone were compared with the results from some of the present tests made with the complete configurations; under conditions in which the afterbodies of the complete models were clear of the water, the resistance was found to be negligibly affected by the presence of the afterbody. Data from the forebody tests were therefore used for some of the models in the speed region where the afterbodies were clear, and only sufficient tests were made with the complete model in this region to determine whether the afterbodies were definitely clear of the water.

RESULTS AND DISCUSSION

The results of the tests are given in figures 3 to 12 in which resistance, trimming-moment, and draft coefficients are plotted against speed coefficient with trim as a parameter. The speed coefficient at which each afterbody cleared the water is indicated in these figures. Unlike the conventional afterbody, which is often wetted by the forebody spray after the afterbody has cleared, the planing-tail afterbodies remained unwetted at all speed coefficients greater than those at which the afterbodies originally cleared.

In order to show the effect of the several parameters under study (depth of step, angle of afterbody keel, length of afterbody chine, and gross load), both best-trim and free-to-trim (zero-trimming-moment) curves were derived for each model. (See figs. 13 to 20.) Free-to-trim resistance characteristics are necessarily a function of the location of the center of gravity. In order to compare free-to-trim data of different hulls, it is therefore necessary to establish a criterion for the selection of the centers of gravity at which the comparisons are to be made. The use of a location of the center of gravity that is a constant distance from some arbitrary point on the model, such as the step, does not always give a fair comparison because the optimum value for this distance may not be the same for each hull. In order to obtain a fair basis for comparing the data for the various configurations, center-of-gravity locations were selected that would result in zero trimming moment for best trim at the speed corresponding to maximum resistance.

Trimming-moment curves at best trim and free-to-trim curves were determined for the same center of gravity. The locations of the center of gravity that resulted from this procedure are given in figures 13 to 20.

Effect of Angle of Afterbody Keel

The effects of angle of afterbody keel on free-to-trim and best-trim characteristics are shown in figures 13 and 14. Figure 21 is a cross plot of resistance coefficient, C_R, against angle of afterbody keel, α, at a constant depth of step, H. Figure 22 is a similar cross plot of C_R against H at values for α of 0° and 4°.

Hump resistance was not greatly affected by change in angle of afterbody keel. At $H = 0.50b$ no appreciable difference was noted in the hump resistance at values of α of 0° and 4° (fig. 22). At $H = 0.35b$ (fig. 21) decreasing α from 6° to 4° had no effect on hump resistance, but a perceptible increase was obtained by reducing α to 0°. Investigations of conventional hulls have generally shown hump resistance to decrease substantially with decreasing angle of afterbody keel. It is logical that if the angle of afterbody keel of any configuration is varied through a sufficiently wide range, an angle that gives minimum hump resistance will be found. This optimum angle would be expected to vary with change in the depth of step and other changes in form. Apparently the range of α that has been of interest in conventional hulls lies above the value of α for minimum hump resistance. In the case of the planing-tail configurations, however, the range of α tested appeared to lie near the value of α for minimum hump resistance; the smallest values of α were below this value for a depth of step of 0.35b. Thus, a tendency for the hump resistance to increase with decreasing angle of afterbody keel may be consistent with the opposite trend found in tests with hulls of conventional form.

The most pronounced effect of varying angle of afterbody keel on free-to-trim resistance (fig. 13) was obtained in the intermediate planing range ($C_V \approx 4.0$) where increasing the angle of afterbody keel caused a large increase in trim above best trim, which resulted in a secondary resistance peak. This peak increased as angle of afterbody keel increased and exceeded the hump resistance at the highest angle of afterbody keel.

Best-trim resistance (figs. 14 and 21) in the speed region $C_V \approx 4.0$ was increased only slightly with increasing angle of afterbody keel. In the high-speed region ($C_V = 6.5$) resistance at best trim was not affected by angle of afterbody keel because the afterbody was clear for all configurations tested and the resistance was essentially that of the forebody alone.

Increasing the angle of afterbody keel increased the trim in the free-to-trim condition throughout nearly all the speed range. The greatest change occurred between values of α of 0° and 2°. (See fig. 13.) Trimming moments for best trim were, in general, greatest at intermediate speeds. The maximum values of trimming moments tended to increase with angle of afterbody keel but the speed at which these maximum values occurred decreased as angle of afterbody keel was increased. (See fig. 14.)

Effect of Depth of Step

The effect of depth of step is shown in figures 15, 16, and 22. The hump resistance was increased by increasing H from 0.35b to 0.50b. In the intermediate planing range, varying the depth of step affected free-to-trim resistance in much the same way as had varying the angle of afterbody keel. Best-trim resistance was little affected at high speeds. The effects obtained for values of α of both 0° and 4° were similar. (See fig. 22.)

An increase in depth of step resulted in an increase in trim in both the best-trim and free-to-trim conditions for all speeds up to that at which the afterbody cleared the water. Trimming moments for best trim were only slightly affected by change in depth of step.

Effect of Sternpost Angle

Sternpost angle σ (fig. 1) is a function of both depth of step and angle of afterbody keel. In figure 23 resistance coefficient is plotted against sternpost angle at three speed coefficients. The secondary peak ($C_V \approx 4.0$) tended to increase with increasing sternpost angle and approximately the same results were obtained whether the

sternpost angle was varied by changing the depth of step or the angle of afterbody keel. At the hump the resistance is not a single-valued function of the sternpost angle. Since the best-trim resistance at high speed ($C_V = 6.5$) was affected by neither depth of step nor angle of afterbody keel, the sternpost angle has no effect on resistance.

Effect of Varying Length of Afterbody Chine

In figures 17 and 18 the effect of varying length of afterbody chine (by omitting the chines for as much as 70 percent of the length of the afterbody) is shown. The part of the afterbody over which the chines are omitted is designated A and the part over which the chines are retained is designated B. The curves show that omitting the chines for the forward 25 percent (1.00b) of the afterbody had no appreciable effect on resistance. Omitting the forward 70 percent (2.80b) of the chines caused the hump resistance to occur at a higher speed, broadened the hump, but had almost no effect on the maximum resistance.

With 70 percent of the chine removed, spray rose as high as 1/2 beam above the afterbody and would tend to be thrown against the tail surfaces with enough force to increase maintenance difficulties.

Effect of Varying Gross Load

The effect of varying gross load on a planing-tail hull is shown in figures 19 and 20; in figure 24 load-resistance ratio Δ/R at best trim is plotted against load coefficient for three speed coefficients. Figure 24 also includes values of Δ/R at best trim for a representative conventional hull (hull A).

The changes in trim and trimming moment caused by increasing the load coefficient were inconsistent but, in general, not large (figs. 19 and 20).

Figure 24 shows that Δ/R at the hump for the planing-tail hull decreased rapidly with increasing load coefficient. At speed coefficients of 4.0 and 6.5, Δ/R for the planing-tail hull was a maximum for the load corresponding to a gross load coefficient of 1.00 and was slightly less at lighter and heavier loads.

This trend differs somewhat from that of conventional hulls. At $C_V = 4.0$, Δ/R for the conventional hull decreased rapidly with increasing load coefficient but at $C_V = 6.5$, Δ/R increased rapidly.

Comparison of Conventional and Planing-Tail Hulls

A comparison of the resistance characteristics of a planing-tail hull (model 163A-11) with those of a conventional hull (hull A) is given in figure 25, in which speed coefficient is plotted against resistance coefficient at best trim for both hulls and against resistance coefficient at free to trim for the planing-tail hull. In the best-trim condition, model 163A-11 had considerably lower resistance than hull A at the hump and at high speeds; at intermediate speeds there is little difference in resistance. In the free-to-trim condition, model 163A-11 had lower resistance than hull A in the best-trim condition over the parts of the speed range where resistance is critical (hump and high speed). At the intermediate speeds, the free-to-trim resistance of the planing-tail hull is somewhat greater than the best-trim resistance of the conventional hull because of high trims.

The foregoing comparison has been made on a basis of equal beams for the two hulls. Actually, model 163A-11 has a greater forebody length-beam ratio than hull A, although the forebody of hull A has the greatest length-beam ratio (3.6) that is in present use on American flying boats.

In figure 26 Δ/R at the hump is plotted against forebody length-beam ratio L_f/b for two series of hulls for which length-beam ratio was varied systematically (unpublished data). The values of Δ/R at the hump for two planing-tail hulls and two unrelated conventional hulls are also plotted in this figure. Figure 26 shows that the values of Δ/R at the hump for all the conventional hulls fall on two rather clearly defined curves, although two of the hulls had no relation to either length-beam series. The values of Δ/R at the hump for the planing-tail hulls are far above the curves.

The increase in Δ/R that would be obtained for hull A by increasing the forebody length-beam ratio is

therefore a small part of the difference in the values of Δ/R for hull A and the planing-tail hulls. The remaining part of the difference must be due to other features peculiar to the planing-tail hull.

The curves of figure 27 show that the low resistance obtained from a planing-tail hull is primarily due to the effectiveness of the planing-tail afterbody. In this figure resistance coefficient, trim, load-resistance ratio, and percentage of total load on the model carried by the afterbody are plotted against speed coefficient for both model 163A-11 and hull B. Curves of Δ/R are given for the forebodies and afterbodies separately as well as for the complete models. Hull B (NACA model 126B-1, reference 4), which is similar to an existing flying boat except for an angle of afterbody keel that is 2° lower, is used in the present comparison because the data were available from unpublished tests. In these tests a special balance was used to measure separately the forces on the forebody and the afterbody. Separation of forces on the forebody and the afterbody of the planing-tail hull was made by the method of reference 1, which uses results of tests made with the forebody alone.

The resistance hump for model 163A-11 occurred at a speed coefficient of 1.8. At this speed the resistance of the two hulls is not greatly different. However, at a speed coefficient of 3.0, at which the resistance hump of hull B occurs, the resistance of model 163A-11 is very much less and the cause of the difference between the resistance curves of the two models at this point is of primary interest. Figure 27(c) shows that at $C_V = 3.0$, the value of Δ/R for the forebody of model 163A-11 is greater than the value for the forebody of hull B (5.1 compared with 4.5). Figure 26 indicates that this difference is due primarily to the difference in length-beam ratios of the two forebodies (4.0 and 3.0). The significant point, however, is that at this speed coefficient ($C_V = 3.0$) the value of Δ/R for the complete hull B is only slightly greater than the value of Δ/R for its forebody, whereas the value of Δ/R for the complete model 163A-11 is notably greater than that for its forebody (6.3 compared with 5.1).

At speed coefficients less than 3.1, the afterbodies of both hulls have higher values of Δ/R than the forebodies. In the speed range in which the greatest

differences in resistance for the two hulls exist, however, the values of Δ/R for the afterbody of model 163A-11 are substantially greater than those for the afterbody of hull B.

When the afterbody has a higher load-resistance ratio than the forebody, it is obviously desirable to carry as much load on the afterbody as possible. Figure 27(d) shows that for values of C_V below 2.5, the conventional hull carries a greater percentage of load on the afterbody than does the planing-tail hull. The load-resistance ratio for the planing-tail afterbody, however, is greater than for the conventional afterbody and compensates for the differences in load carried by the two afterbodies to such an extent that the resistance of the planing-tail hull is the lower over part of this speed range.

At speed coefficients greater than 2.5, the planing-tail afterbody not only carries a greater percentage of load than does the conventional afterbody but also maintains a greater load-resistance ratio. These two characteristics of the afterbody of the planing-tail hull are the primary causes for the reduction of resistance at the speeds at which hump occurs for the conventional hull. It is notable that the planing-tail hull maintains a higher value of Δ/R while operating at a lower trim (fig. 27(b)).

In general, the best trim for the complete model 163A-11 is the same as the best trim for its forebody. It is remarkable that, when the forebody is operating at its best trim, the afterbody has much greater values of Δ/R than has the forebody. At speed coefficients between 2.0 and 3.5, the values of Δ/R for a highly efficient planing surface with straight buttocks were found in reference 1 to be less than 6. The afterbody of model 163A-11 has values of Δ/R several times this value in the same speed range. Over most of this speed range, even the conventional afterbody has values of Δ/R greater than 6. These afterbodies, therefore, carry load with less resistance than would a single planing surface running in undisturbed water. In order to obtain this result, some energy of the forebody wake must be converted into useful lift, which is more effectively accomplished by the planing-tail afterbody than by the conventional afterbody.

CONCLUSIONS

Results of tank tests to determine the effect of varying design parameters of planing-tail hulls led to the following conclusions:

1. The effect of varying design parameters indicated

(a) Increasing the angle of afterbody keel had small effect on hump resistance but produced a secondary peak in the curves of free-to-trim resistance at the intermediate planing range. At best trim only a slight increase in resistance at planing speeds was noted as angle of afterbody keel was increased. Angle of afterbody keel had no effect on high-speed resistance.

(b) Increasing the depth of step increased hump resistance. Free-to-trim resistance in the intermediate planing range was increased in a similar manner for depth of step as for angle of afterbody keel. Best-trim resistance was little affected at high speeds.

(c) Omitting the chines on the forward 25 percent of the afterbody had no appreciable effect on resistance. Omitting the forward 70 percent of the chines caused the hump to occur at a higher speed, broadened the hump, but had almost no effect on maximum resistance. Spray around the afterbody increased with 70 percent of the chines removed.

(d) Load-resistance ratio at the hump decreased more rapidly with increasing load coefficient for the planing-tail hull than for the representative conventional hull, although the load-resistance ratio at the hump was greater for the planing-tail hull than for the conventional hull throughout the range of loads tested. At speeds higher than hump speed, load-resistance ratio for the planing-tail hull was a maximum at a particular gross load and was slightly less at heavier and lighter gross loads.

2. A comparison of a planing-tail and a conventional hull showed

(a) The planing-tail hull had lower best-trim resistance at the hump and at high speed with little difference in resistance throughout the intermediate planing range.

(b) The planing-tail hull had lower free-to-trim resistance than the best-trim resistance of the conventional hull at the hump and at high speed with higher resistance in the intermediate planing range.

(c) The planing-tail hull had lower hump resistance primarily because of the ability of its afterbody to take a greater percentage of the total load while maintaining a higher load-resistance ratio than the conventional afterbody.

Langley Memorial Aeronautical Laboratory
National Advisory Committee For Aeronautics
Langley Field, Va., April 30, 1946

REFERENCES

1. Dawson, John R., and Wadlin, Kenneth L.: Preliminary Tank Tests with Planing-Tail Seaplane Hulls. NACA ARR No. 3F15, 1943.

2. Dawson, John R., Walter, Robert C., and Hay, Elizabeth S.: Tank Tests To Determine the Effect of Varying Design Parameters of Planing-Tail Hulls. I - Effect of Varying Length, Width, and Plan-Form Taper of Afterbody. NACA TN No. 1062, 1946.

3. Dawson, John R.: Tank Tests of Three Models of Flying-Boat Hulls of the Pointed-Step Type with Different Angles of Dead Rise - N.A.C.A. Model 35 Series. NACA TN No. 551, 1936.

4. Bell, Joe W., and Willis, John M., Jr.: The Effects of Angle of Dead Rise and Angle of Afterbody Keel on the Resistance of a Model of a Flying-Boat Hull. NACA ARR, Feb. 1943.

TABLE I

PERTINENT MODEL DIMENSIONS AND PARAMETERS

Langley tank model	α (deg)	σ (deg)	H (in.)	A (in.)	B (in.)	x (in.) (a)	C_{Δ_o}
163A-1	0	4.95	4.5	6.0	46.0	1.00	1.00
163A-6	2	6.93	4.5	6.0	46.0	[b]-1.14	1.00
163A-11	4	8.90	4.5	6.0	46.0	1.50	1.00
163A-16	6	10.88	4.5	6.0	46.0	5.40	1.00
163A-3	0	7.13	6.5	6.0	46.0	0.50	1.00
163A-13	4	11.05	6.5	6.0	46.0	4.90	1.00
163A-11A	4	8.90	4.5	13.0	39.0	2.85	1.00
163A-11B	4	8.90	4.5	36.4	15.6	3.60	1.00
163A-11	4	8.90	4.5	6.0	46.0	4.60	0.75
163A-11	4	8.90	4.5	6.0	46.0	4.50	1.25

[a]Locations of center of moments given are ones that give a minimum value for peak resistance with the model free to trim.

[b]Distances measured aft of step are considered negative.

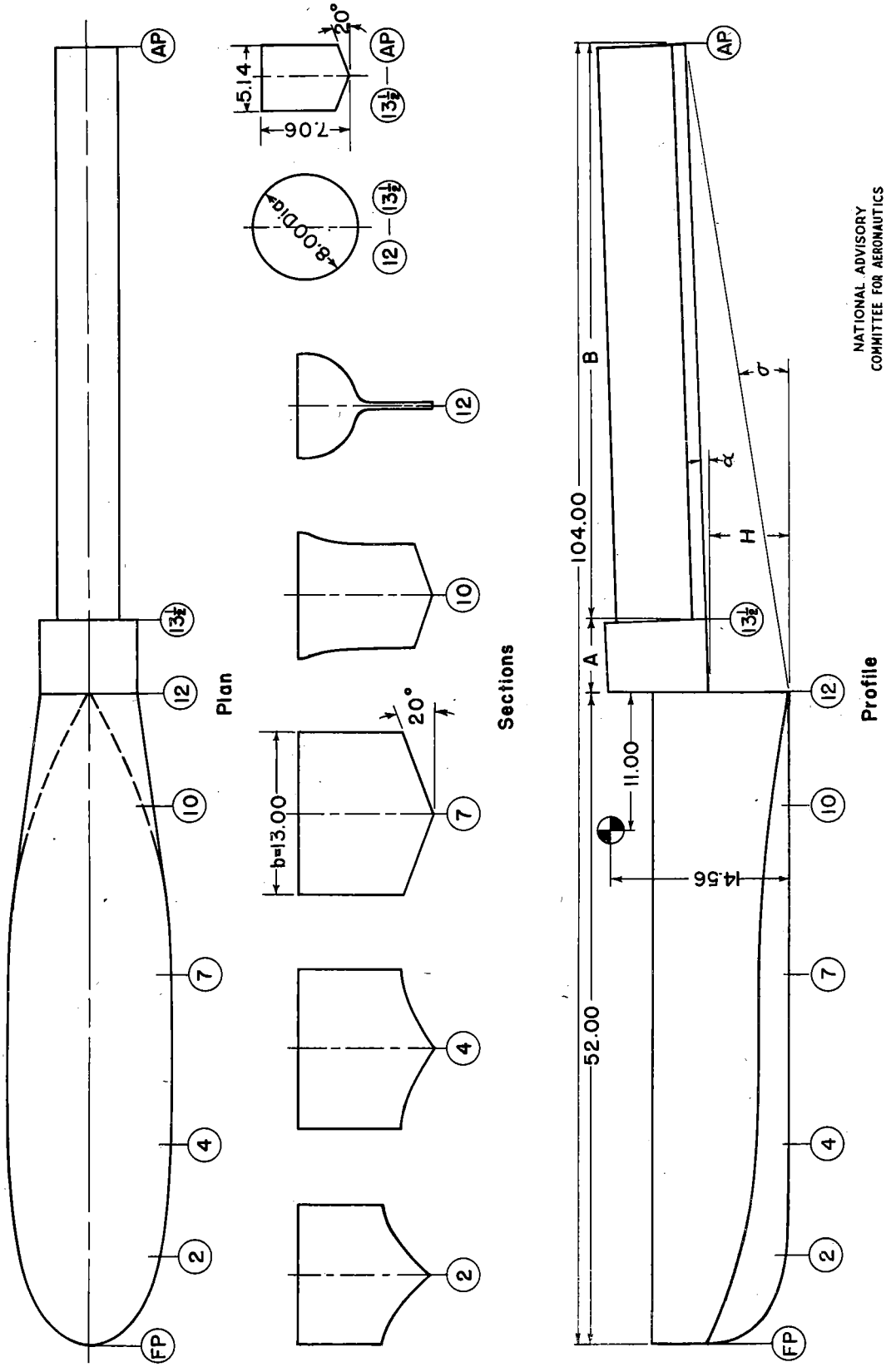

Figure 1-Lines of NACA model 163 A series. (All dimensions are in inches.)

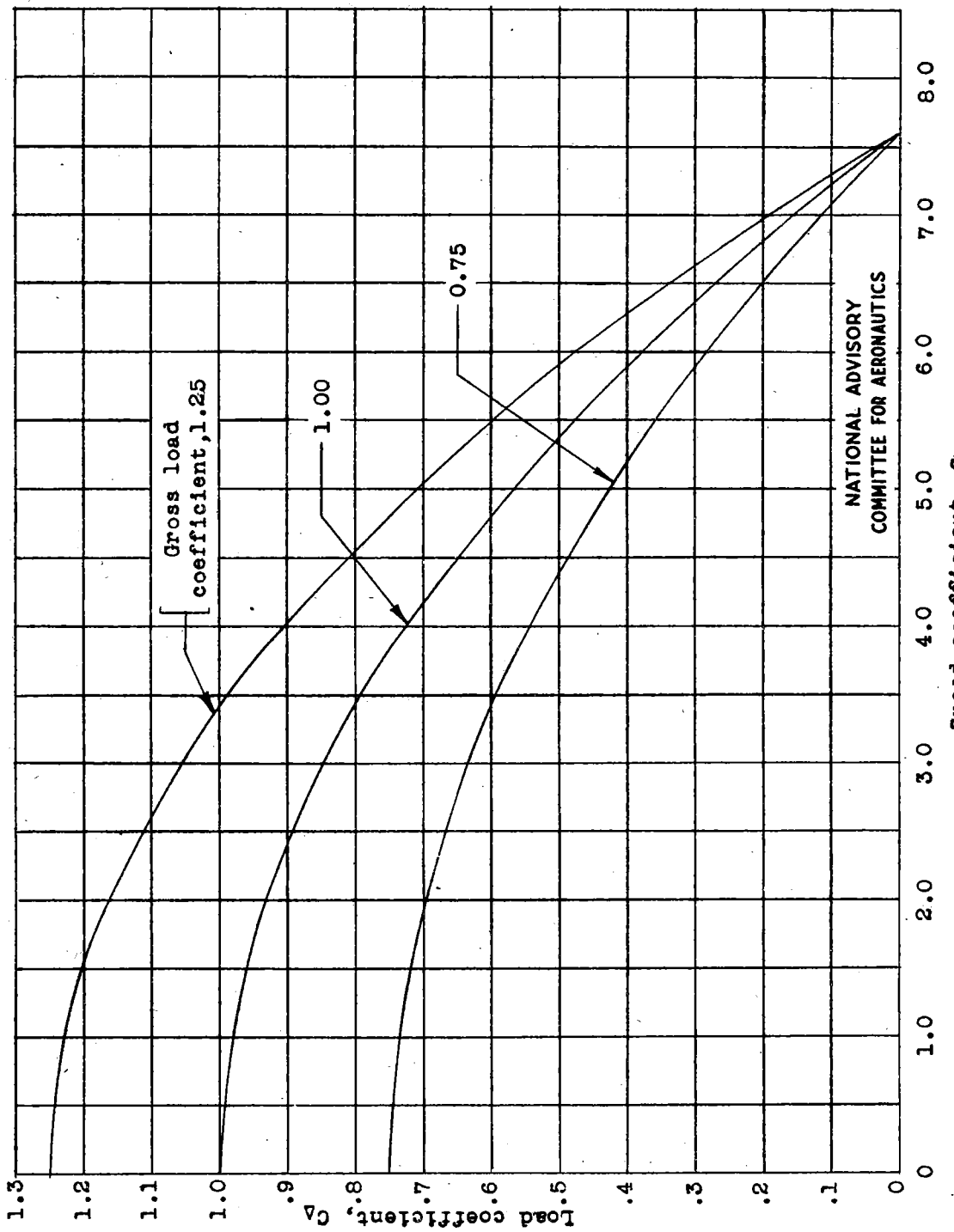

Figure 2.- Load curves for model 163A series.

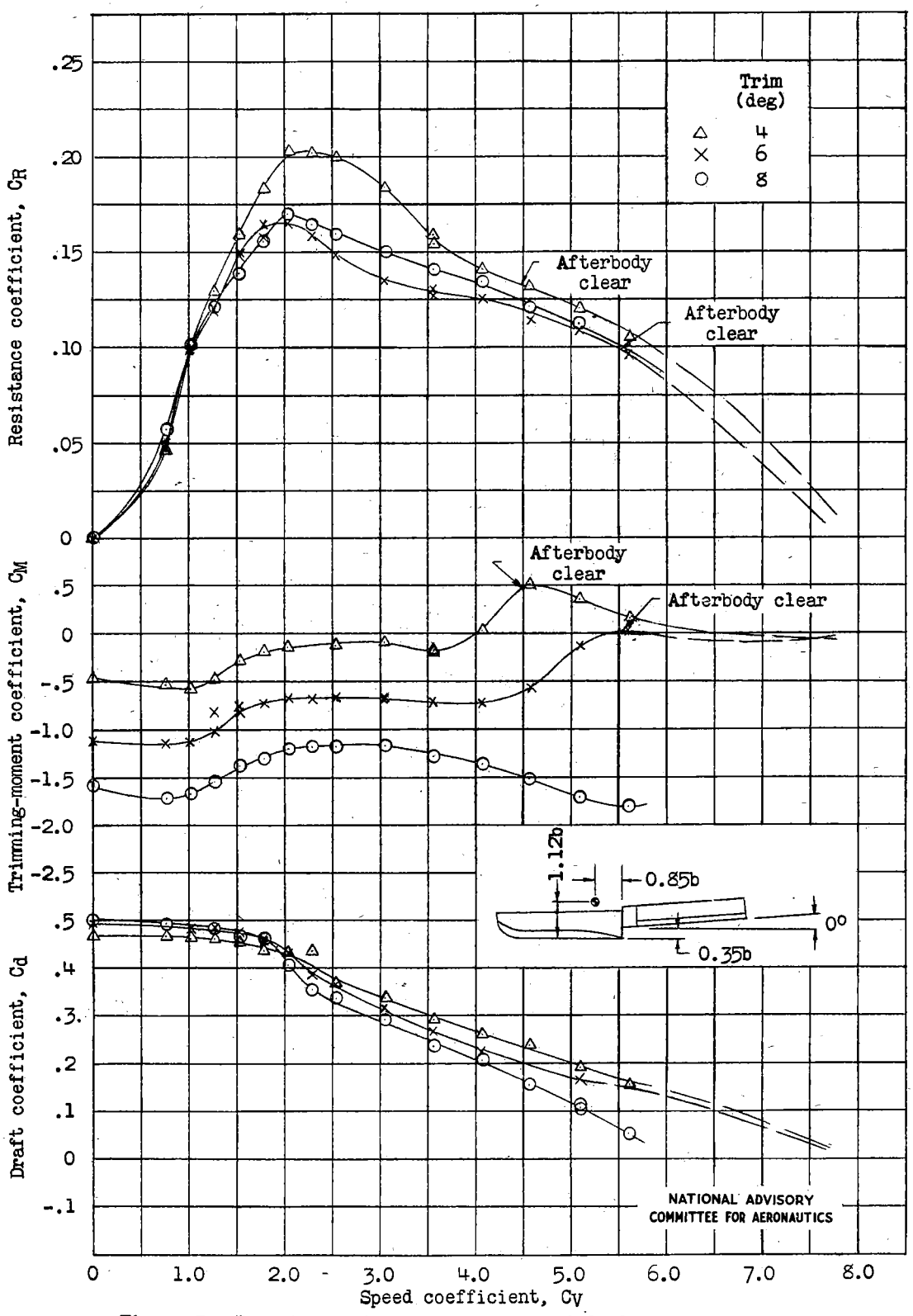

Figure 3.- Resistance, trimming-moment, and draft characteristics of model 163A-1 at fixed trim. Gross load coefficient, 1.00.

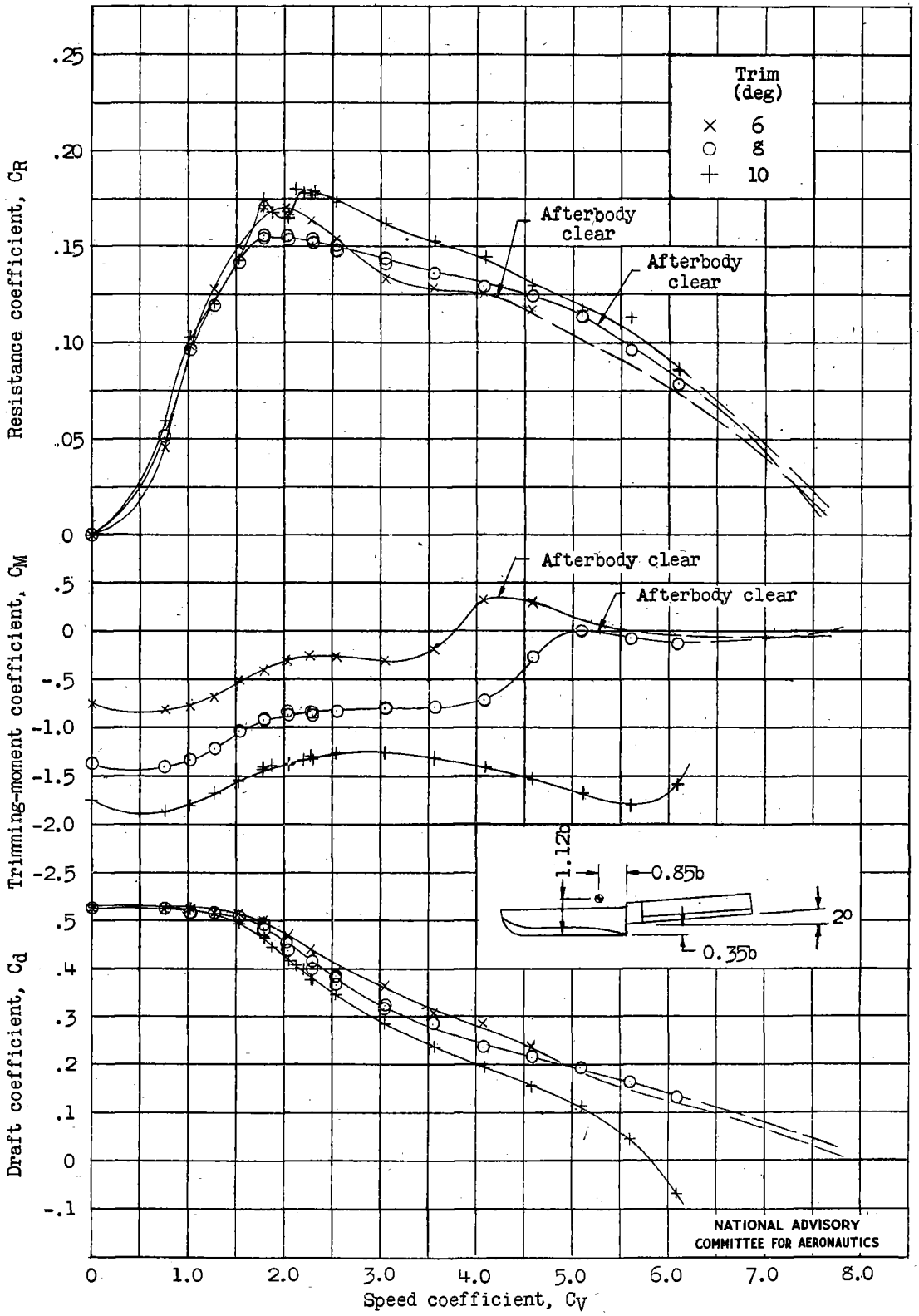

Figure 4.- Resistance, trimming-moment, and draft characteristics of model 163A-6 at fixed trim. Gross load coefficient, 1.00.

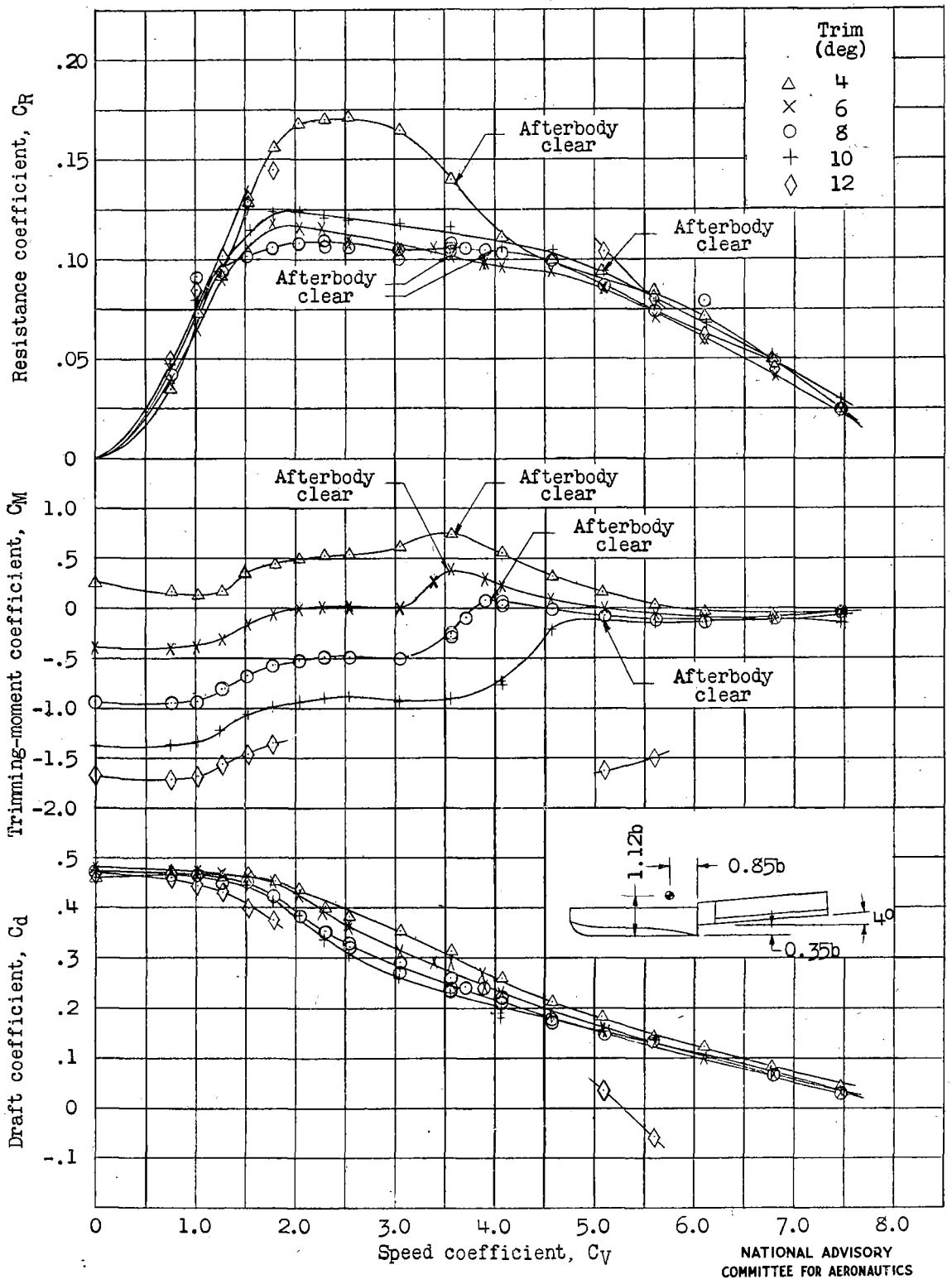

Figure 5.- Resistance, trimming-moment, and draft characteristics of model 163A-11 at fixed trim. Gross load coefficient, 0.75.

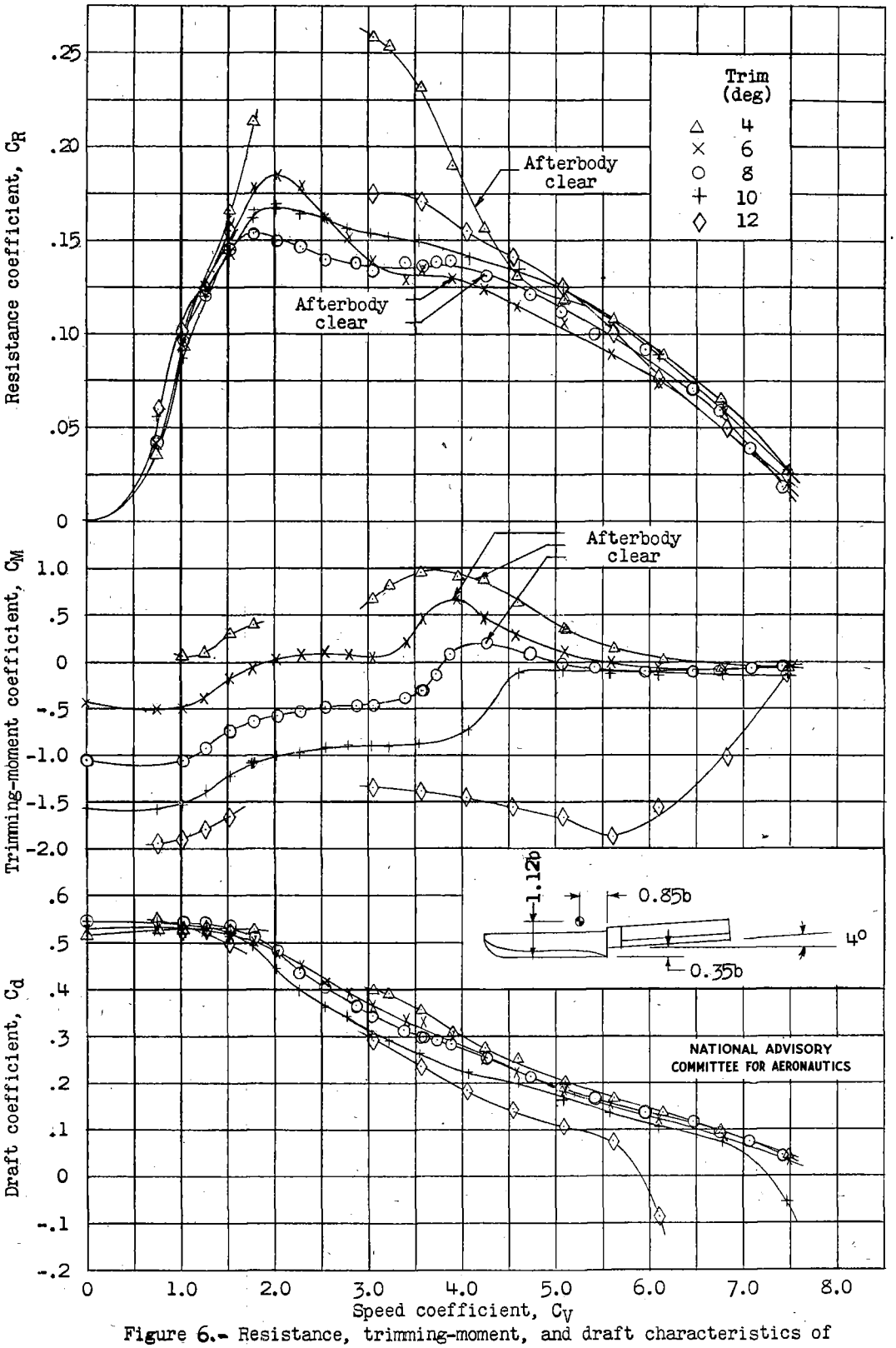

Figure 6.- Resistance, trimming-moment, and draft characteristics of model 163A-11 at fixed trim. Gross load coefficient, 1.00.

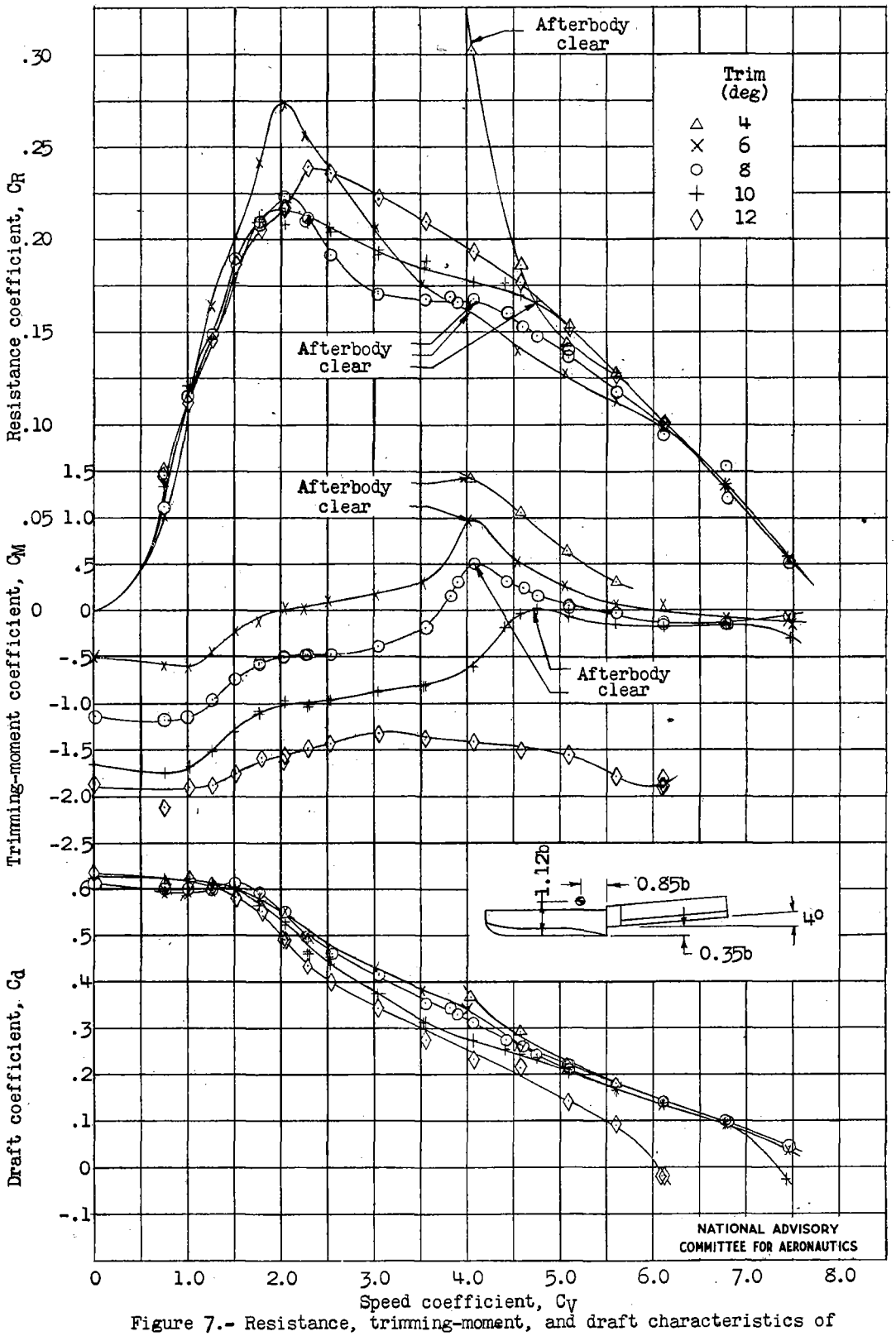

Figure 7.- Resistance, trimming-moment, and draft characteristics of model 163A-11 at fixed trim. Gross load coefficient, 1.25.

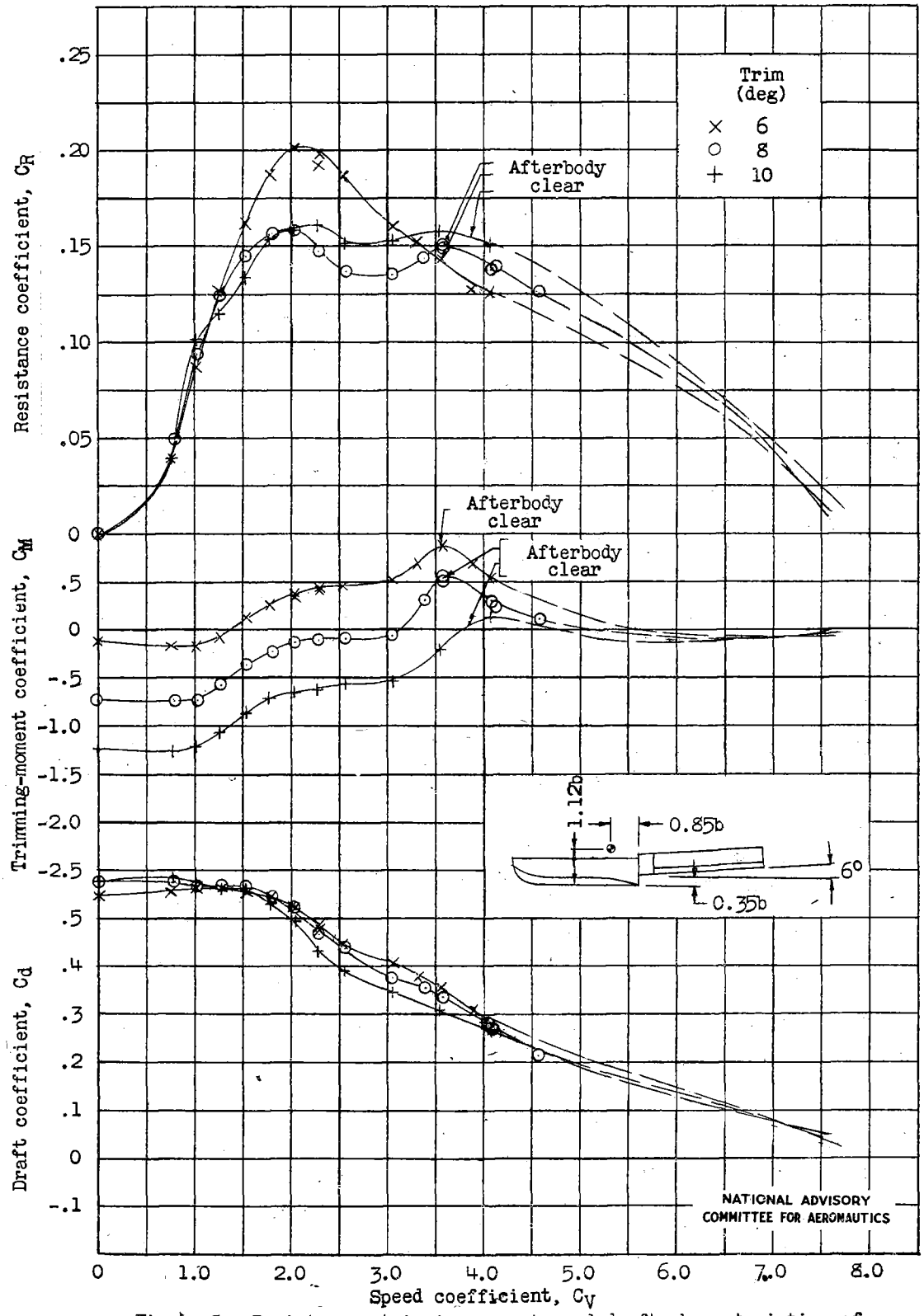

Figure 8.- Resistance, trimming-moment, and draft characteristics of model 163A-16 at fixed trim. Gross load coefficient, 1.00.

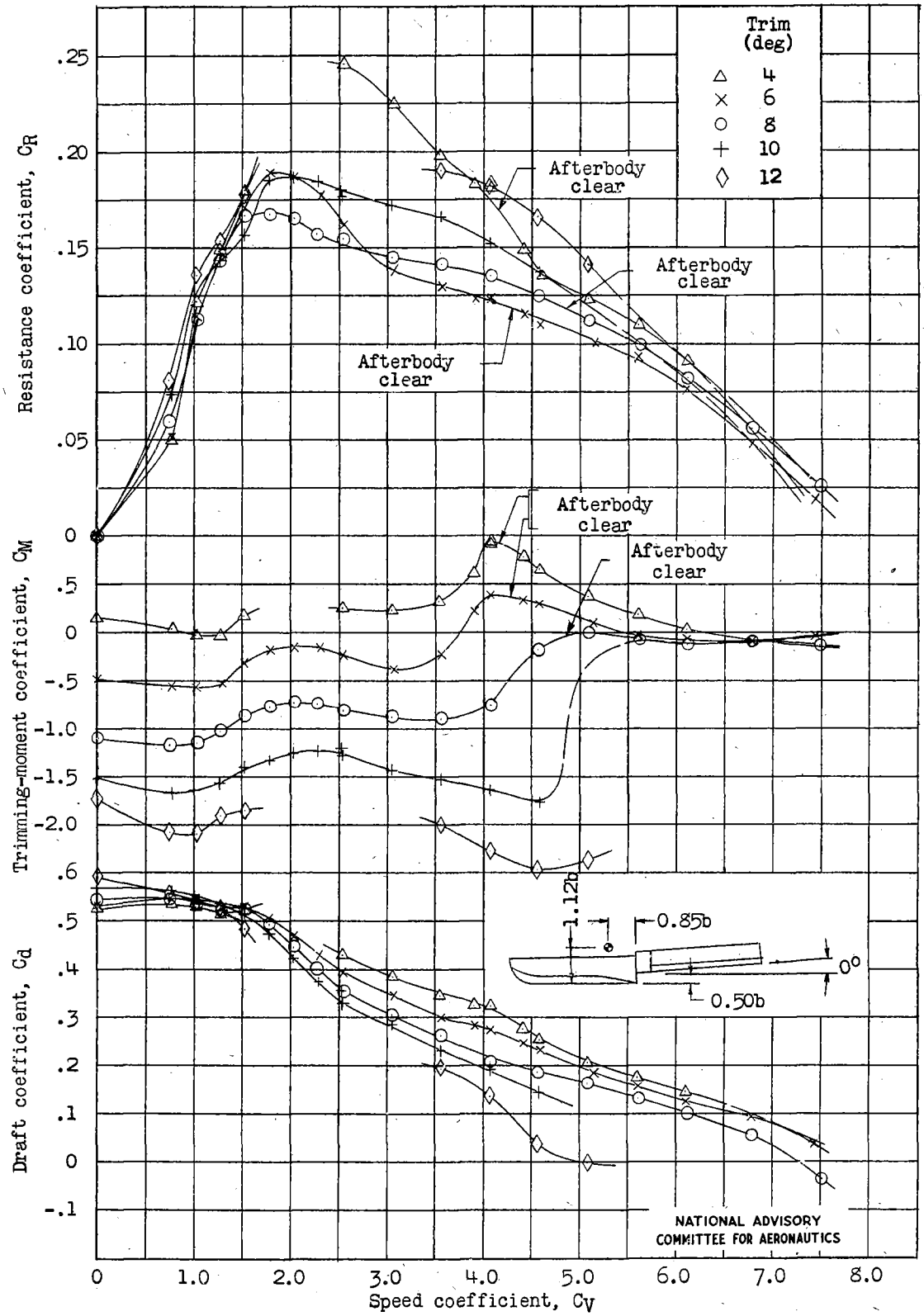

Figure 9.- Resistance, trimming-moment, and draft characteristics of model 163A-3 at fixed trim. Gross load coefficient, 1.00.

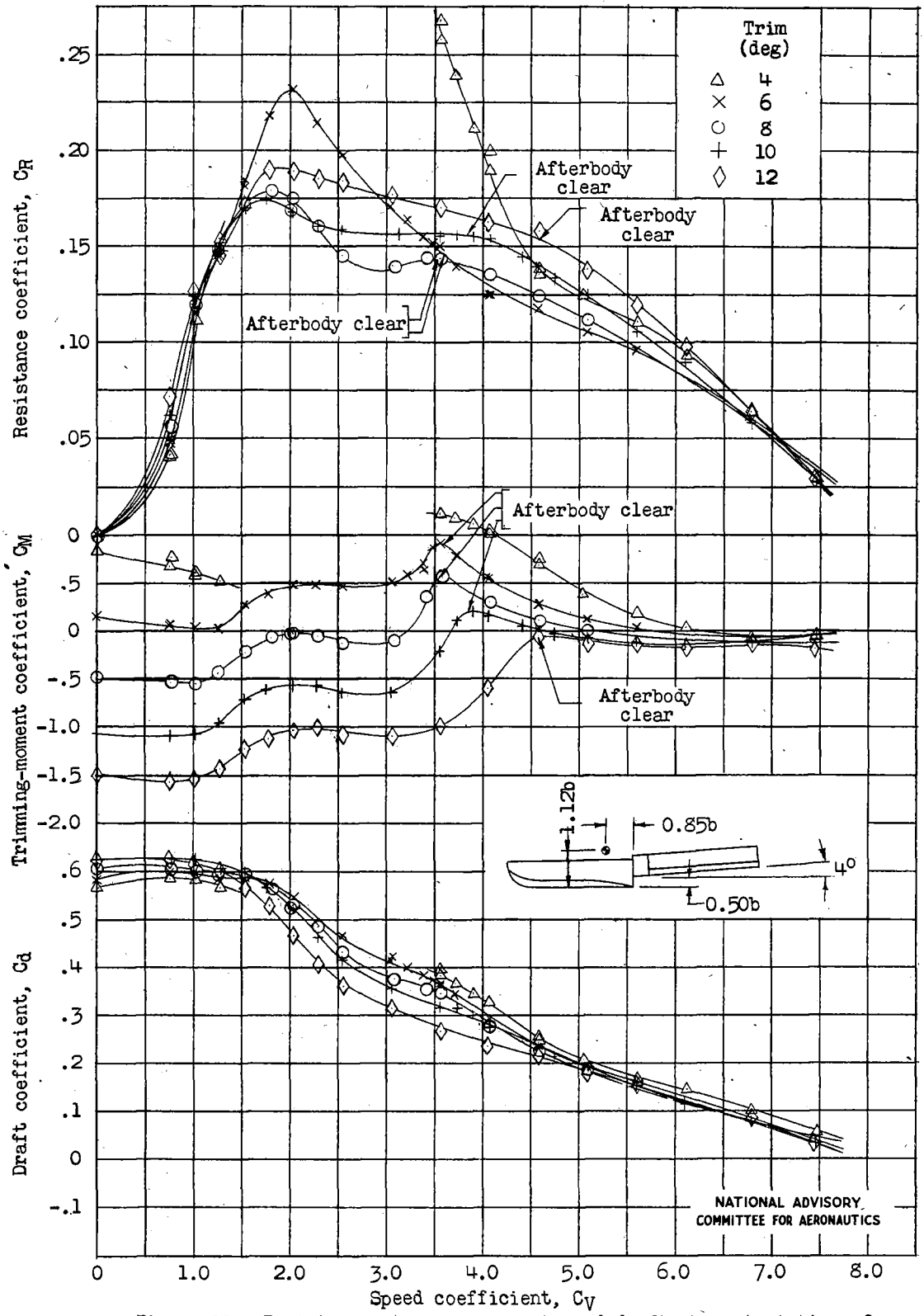

Figure 10.- Resistance, trimming-moment, and draft characteristics of model 163A-13 at fixed trim. Gross load coefficient, 1.00.

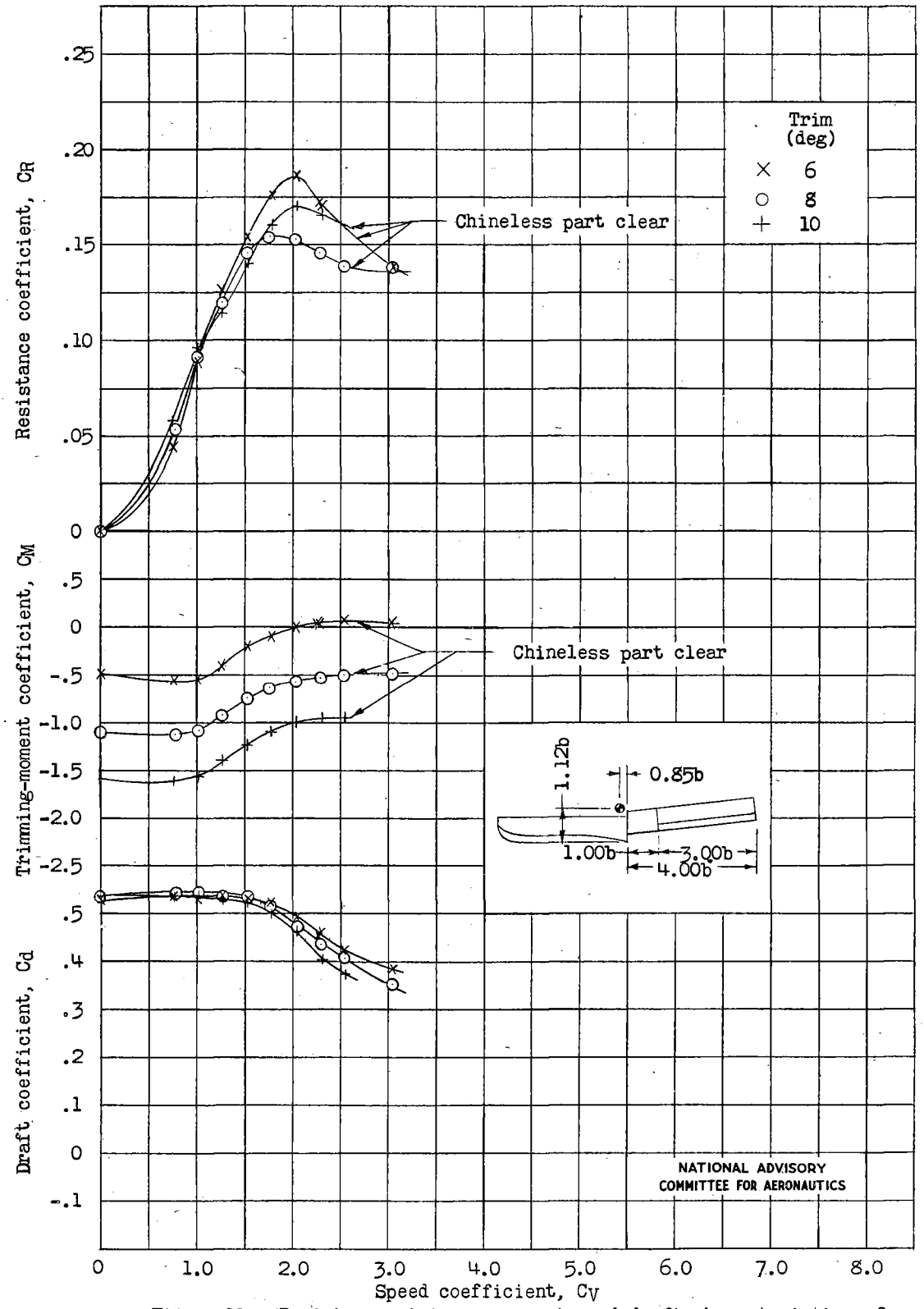

Figure 11.- Resistance, trimming-moment, and draft characteristics of model 163A-11A at fixed trim. Gross load coefficient, 1.00.

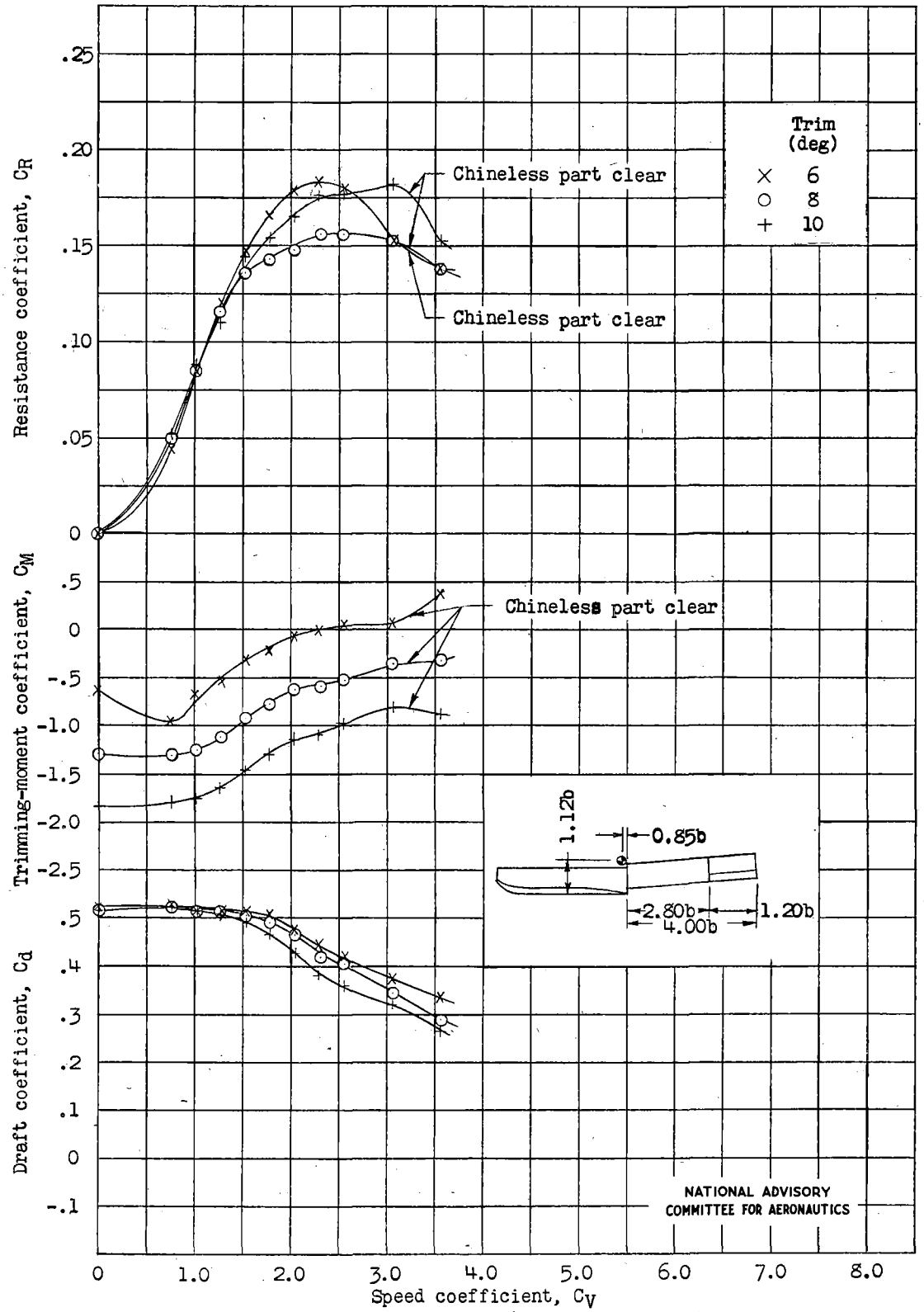

Figure 12.- Resistance, trimming-moment, and draft characteristics of model 163A-11B at fixed trim. Gross load coefficient, 1.00.

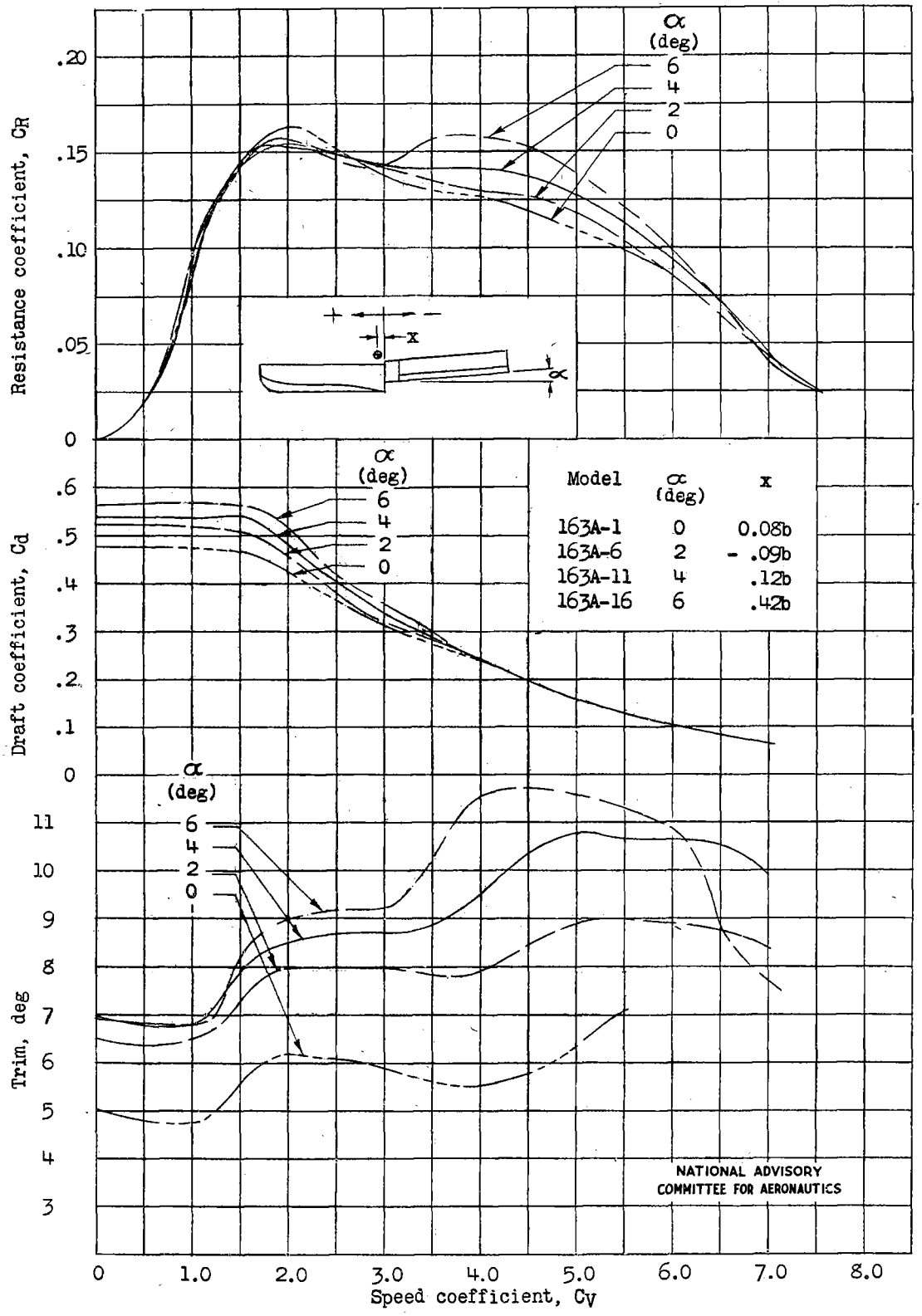

Figure 13.- Effect on free-to-trim characteristics of varying angle of afterbody keel. H = 0.35b; C_{Δ_0} = 1.00.

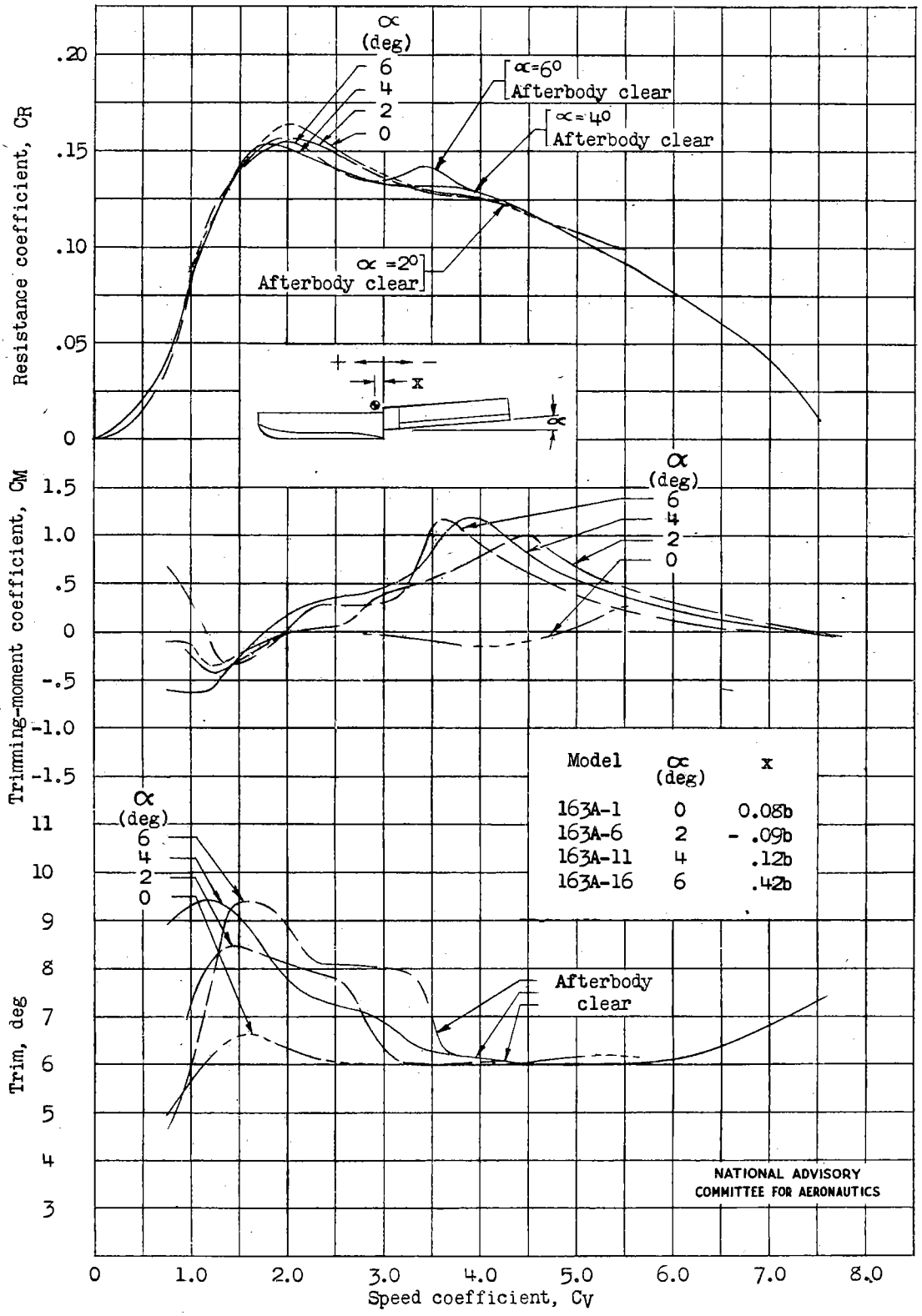

Figure 14.- Effect on best-trim characteristics of varying angle of afterbody keel. H = 0.35b; C_{Δ_C} = 1.00.

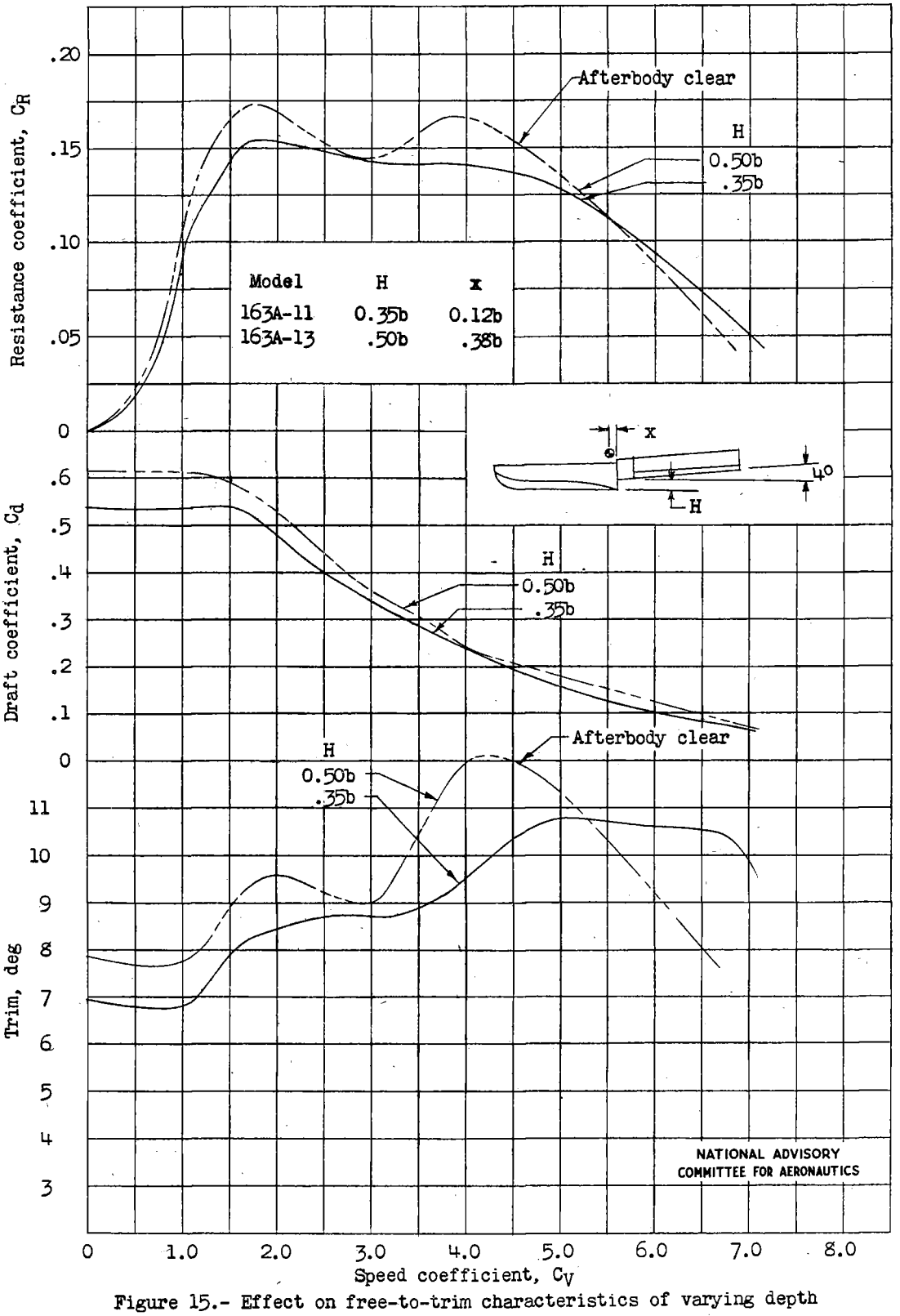

Figure 15.- Effect on free-to-trim characteristics of varying depth of step. $\alpha = 4.0°$; $C_{\Delta_0} = 1.00$.

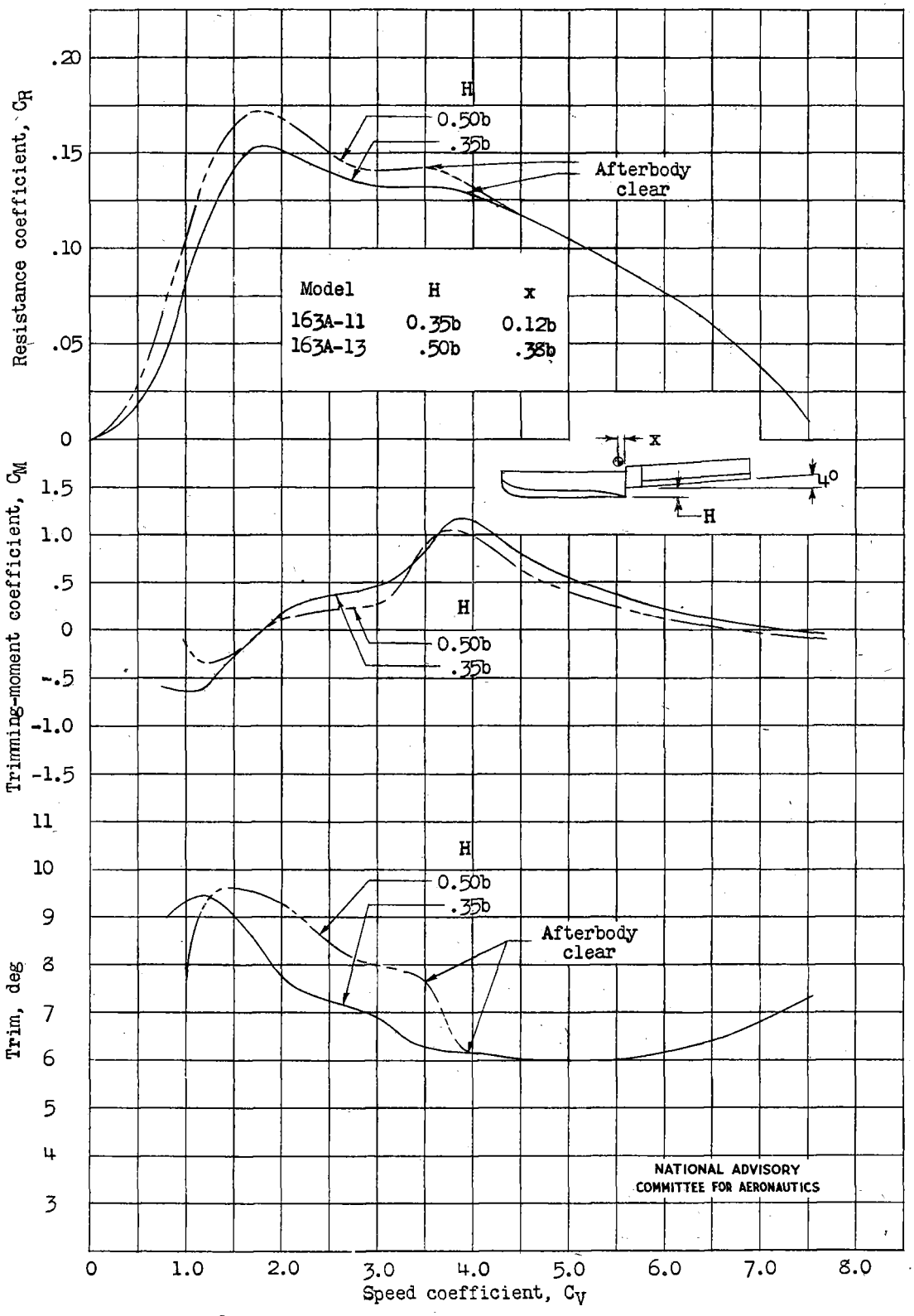

Figure 16.- Effect on best-trim characteristics of varying depth of step. $\alpha = 4.0^\circ$; $C_{\Delta_0} = 1.00$.

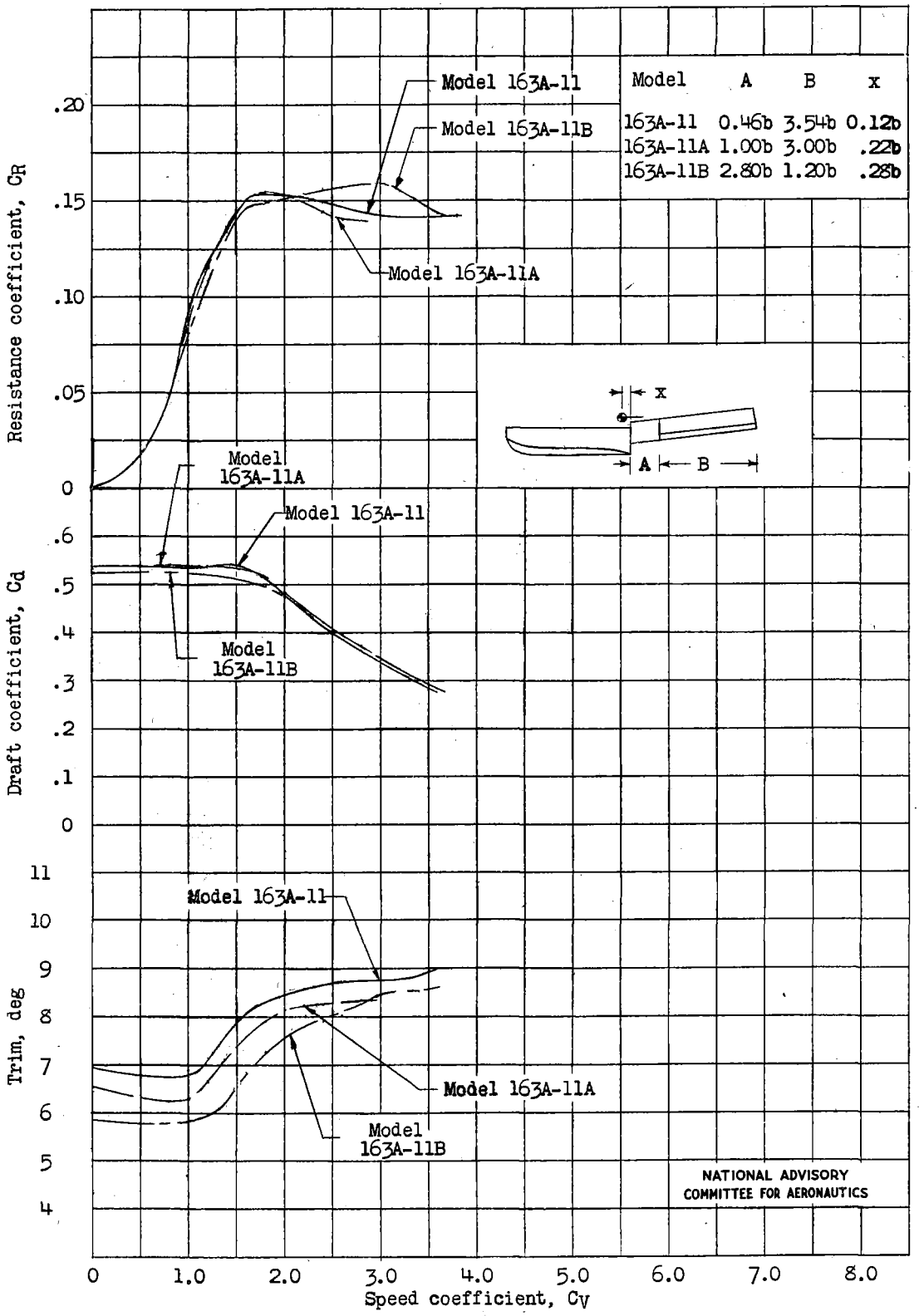

Figure 17.- Effect on free-to-trim characteristics of omitting part of afterbody chines. α = 4.0°; H = 0.35b; C_{Δ_0} = 1.00.

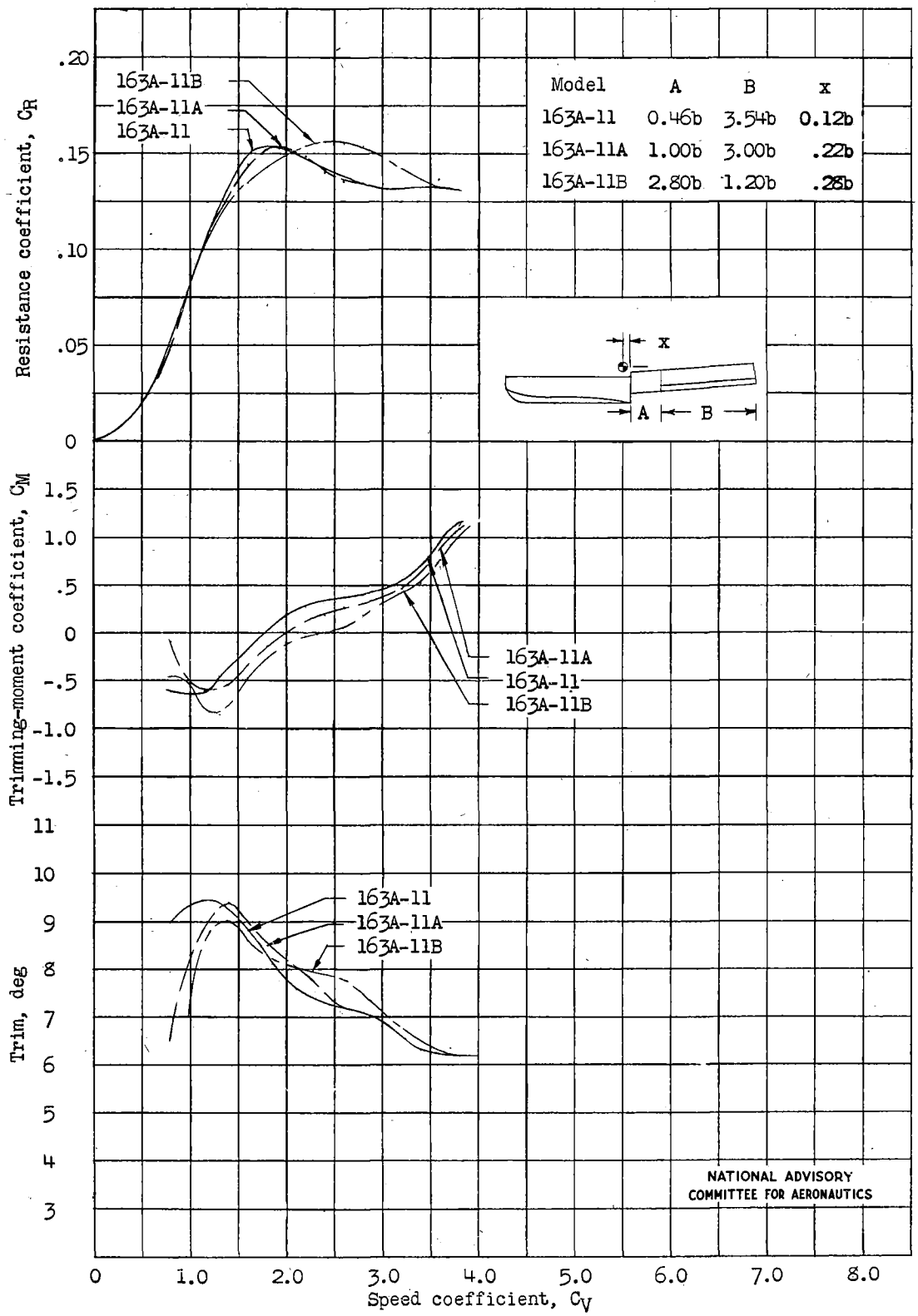

Figure 18.- Effect on best-trim characteristics of omitting part of afterbody chines. $\alpha = 4.0°$; H = 0.35b; $C_{\Delta_0} = 1.00$.

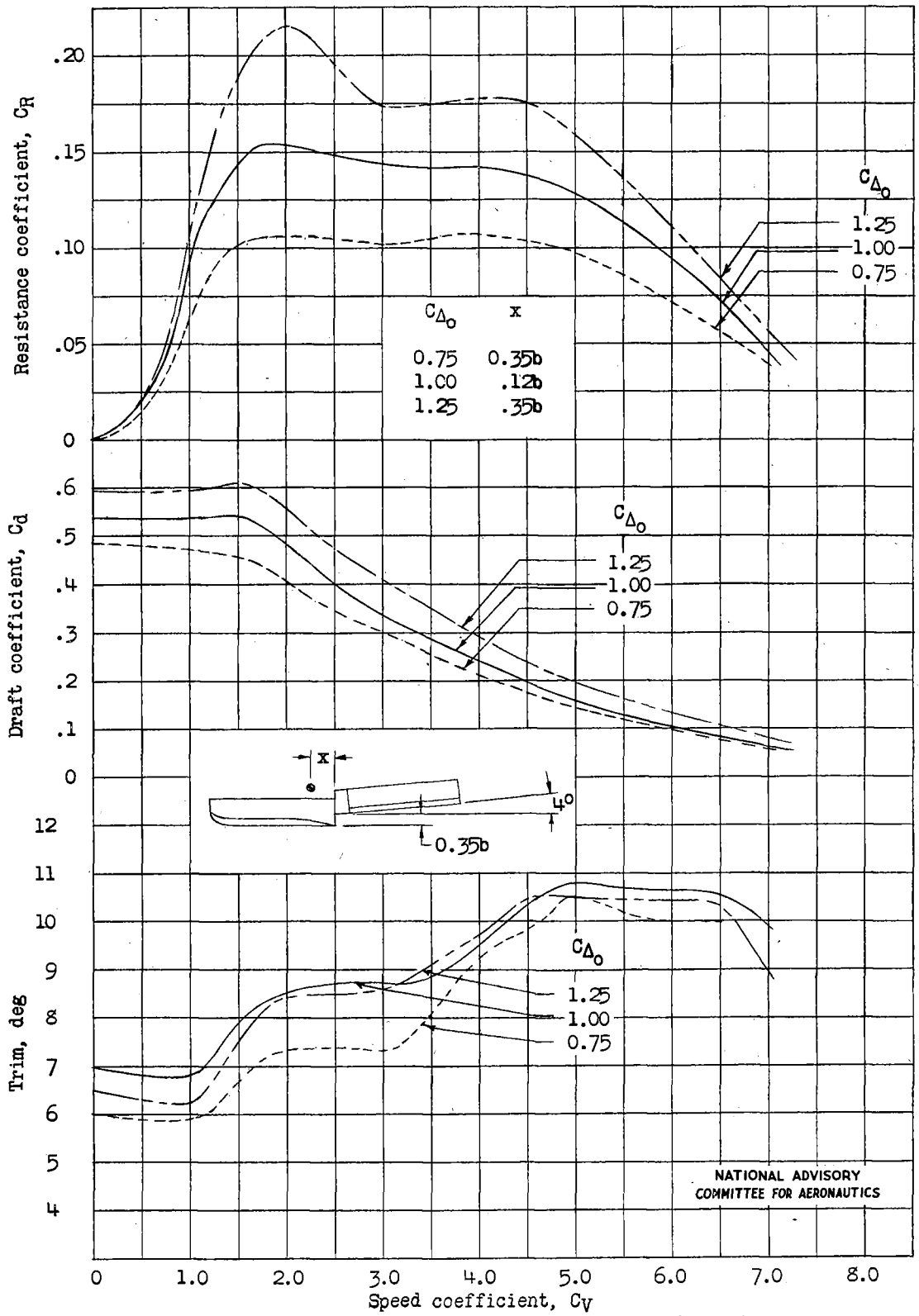

Figure 19.- Effect on free-to-trim characteristics of varying gross load coefficient. Model 163A-11. $\alpha = 4.0°$; H = 0.35b.

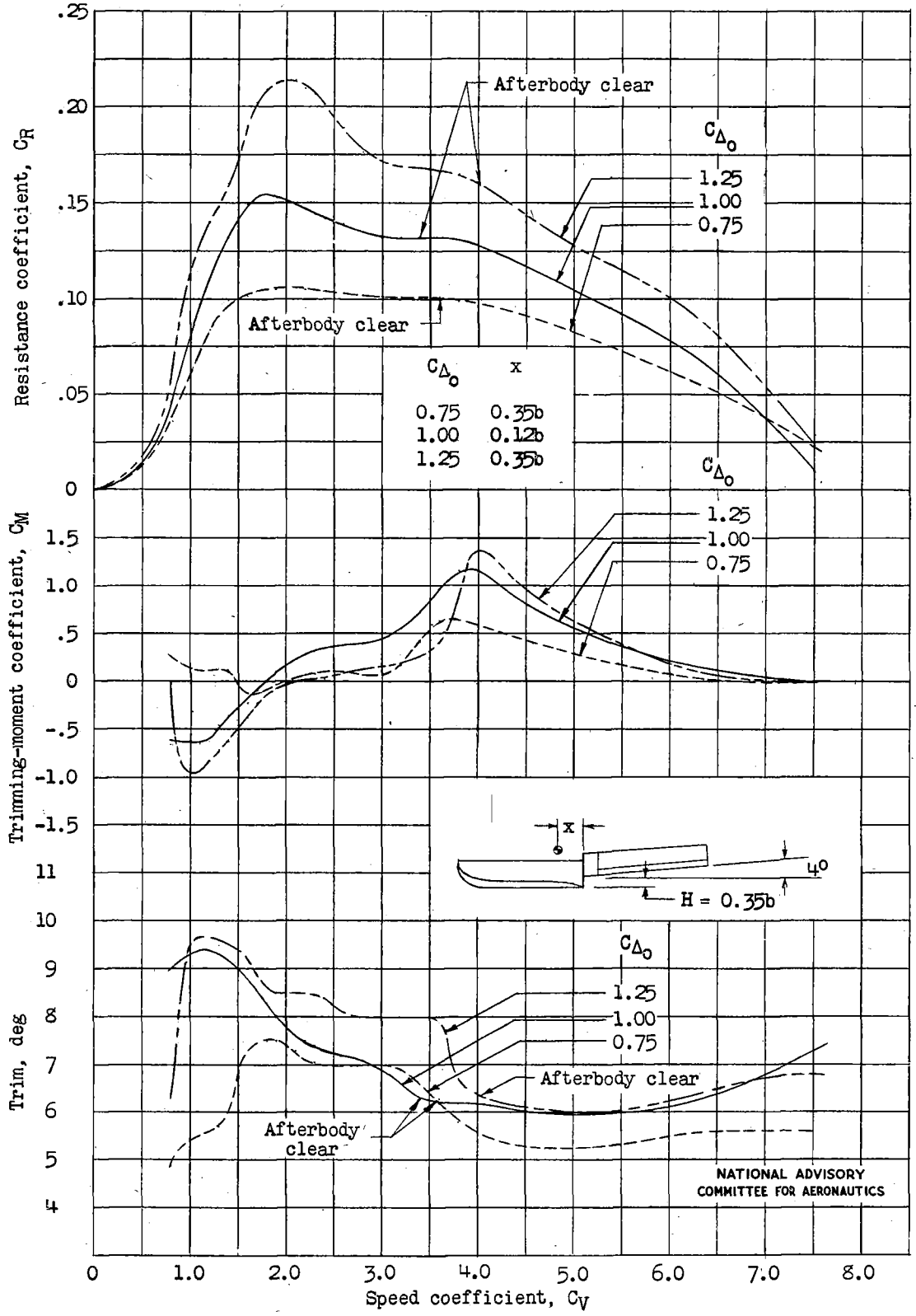

Figure 20.- Effect on best-trim characteristics of varying gross load coefficient. Model 163A-11. α = 4.0°; H = 0.35b.

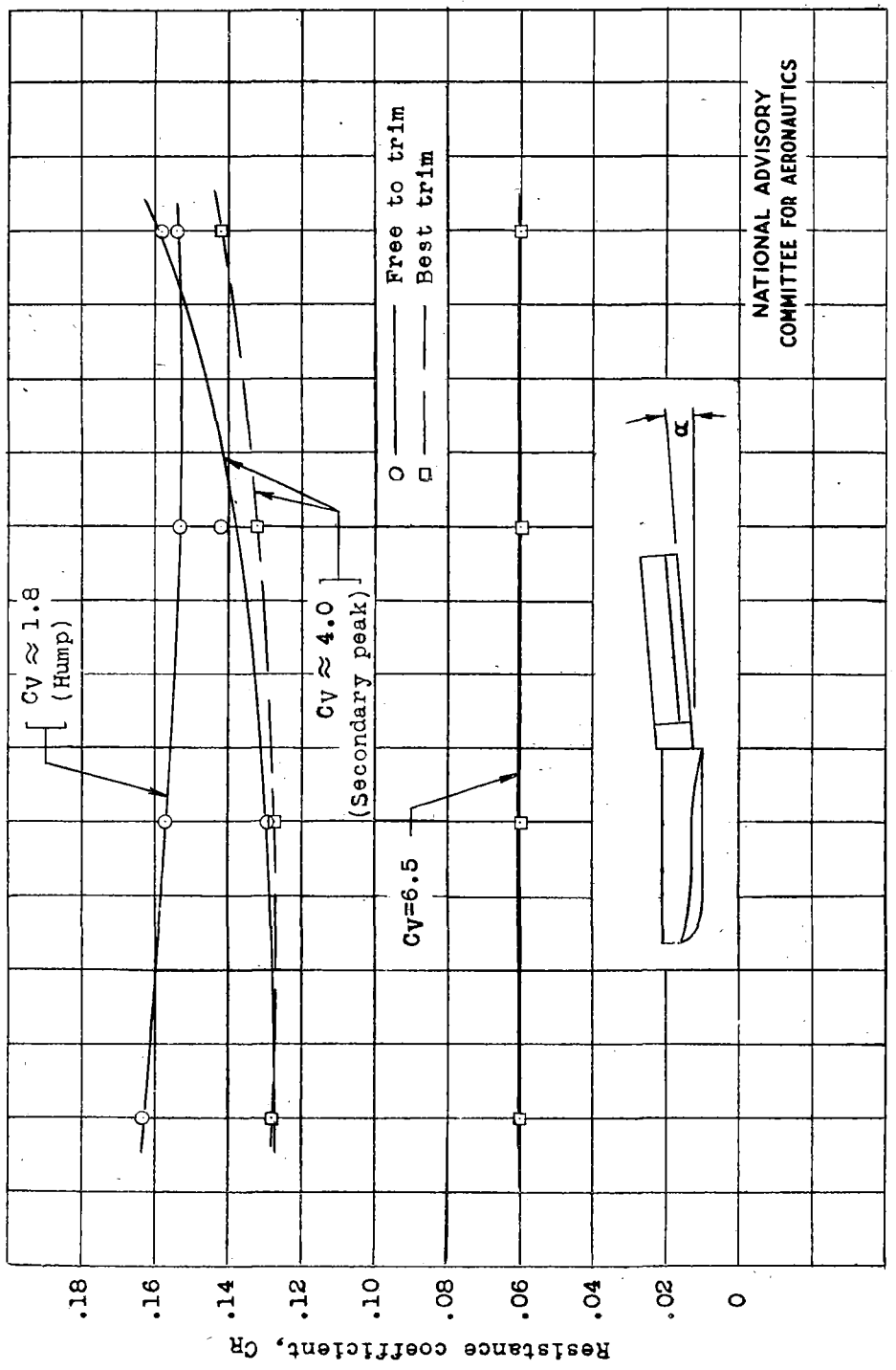

Figure 21.- Effect of angle of afterbody keel on hump resistance, best-trim and free-to-trim resistance at intermediate planing range, and best-trim resistance at high speed. H = 0.35b; C_{Δ_o} = 1.00.

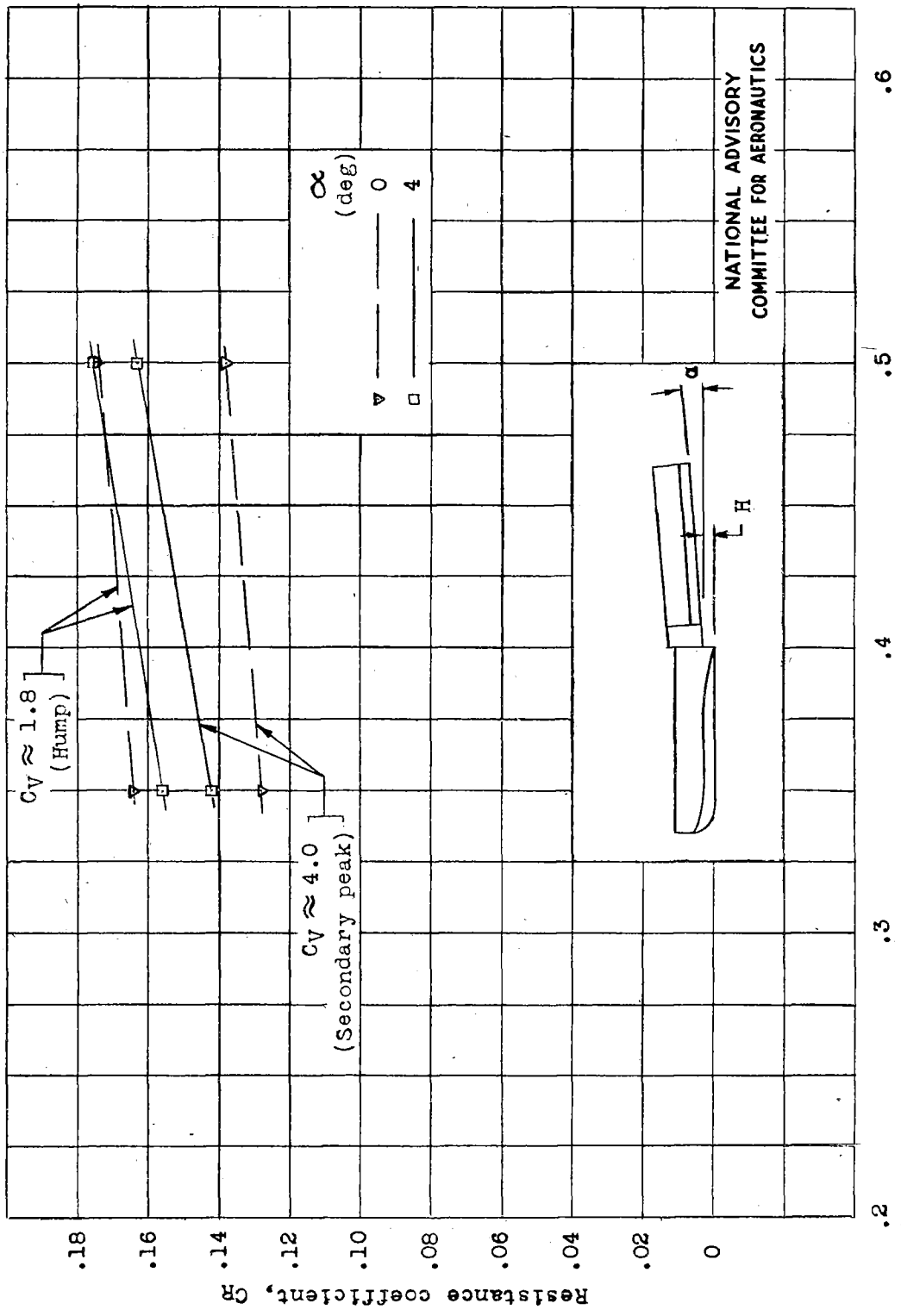

Figure 22.- Effect of depth of step on free-to-trim resistance. $C_{\Delta_o} = 1.00$.

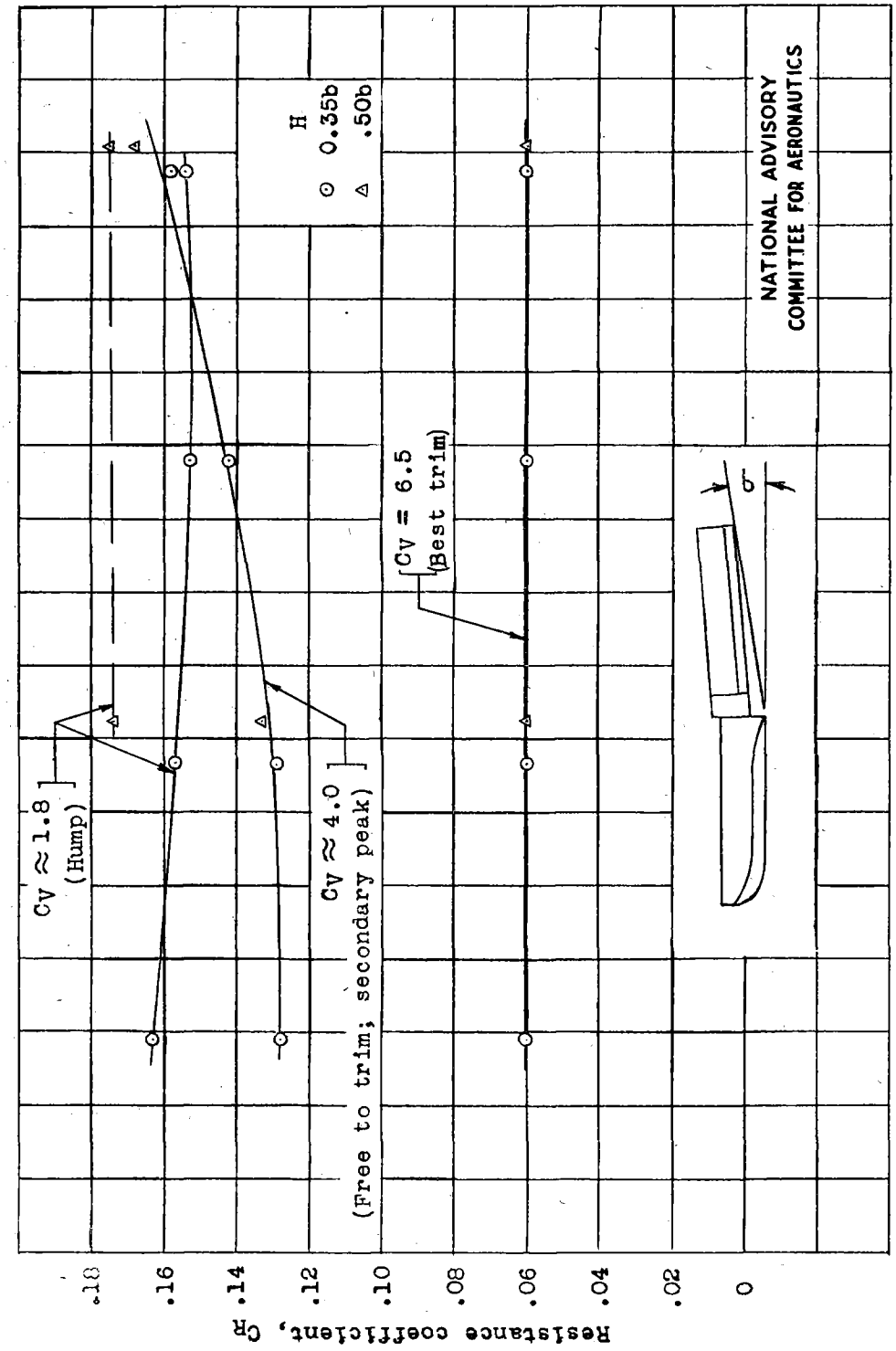

Figure 23.- Effect of sternpost angle on hump resistance, free-to-trim resistance at intermediate planing range, and best-trim resistance at high speed. $C_{\Delta_o} = 1.00$.

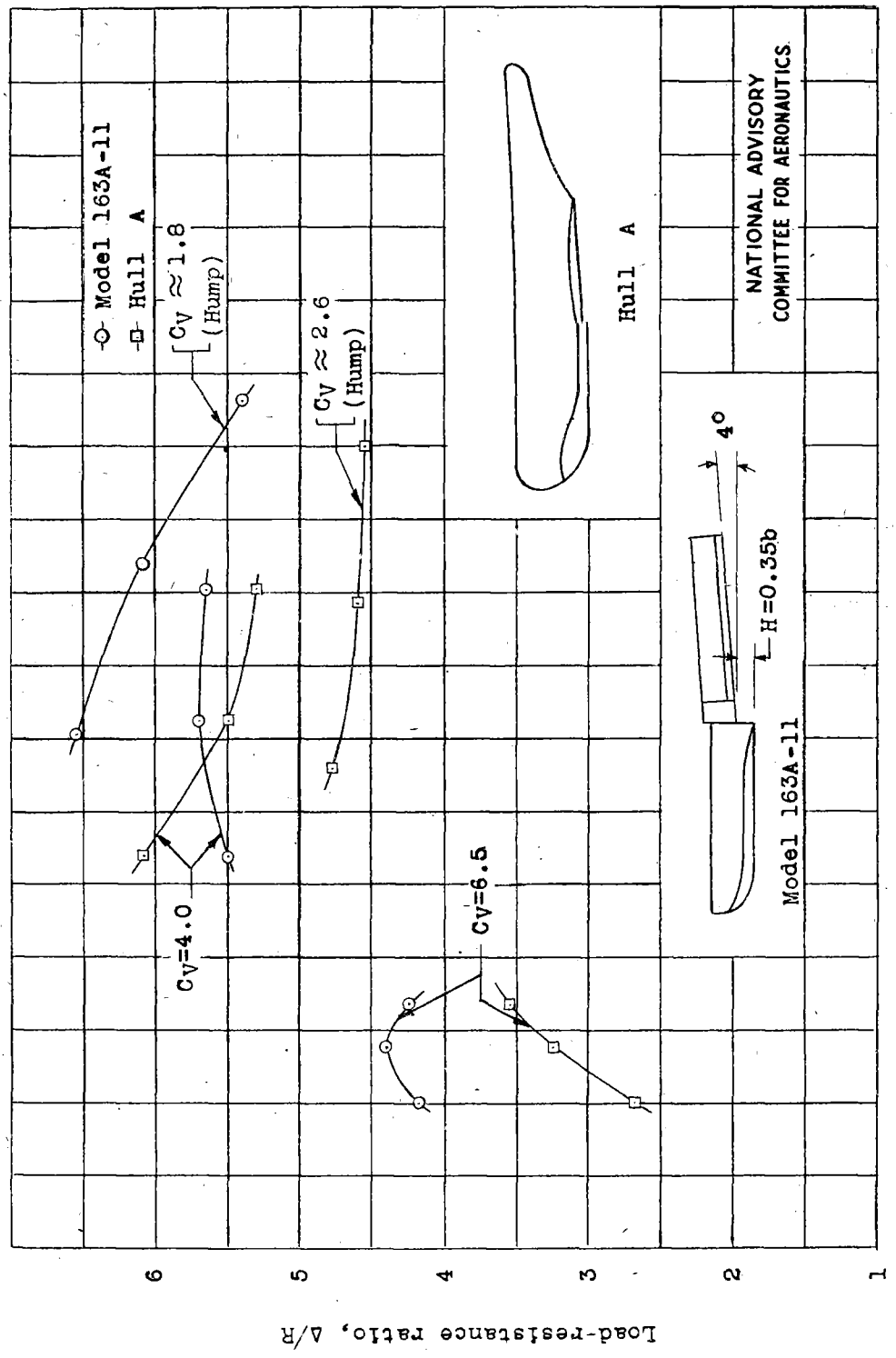

Figure 24.- Comparison of best-trim load-resistance ratios of model 163A-11 and hull A.

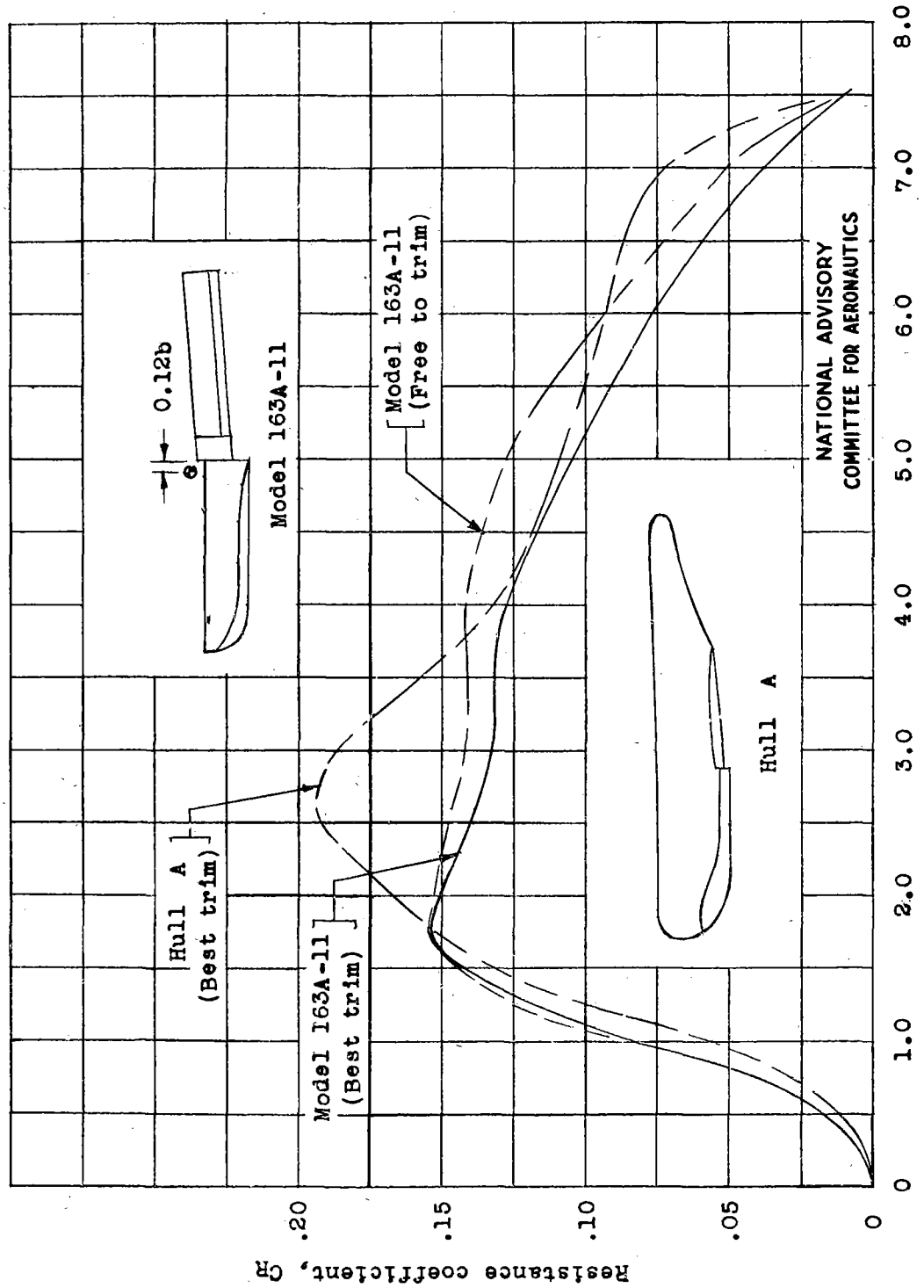

Figure 25.- Comparison of best-trim resistance of hull A with best-trim and free-to-trim resistance of model 163A-11.

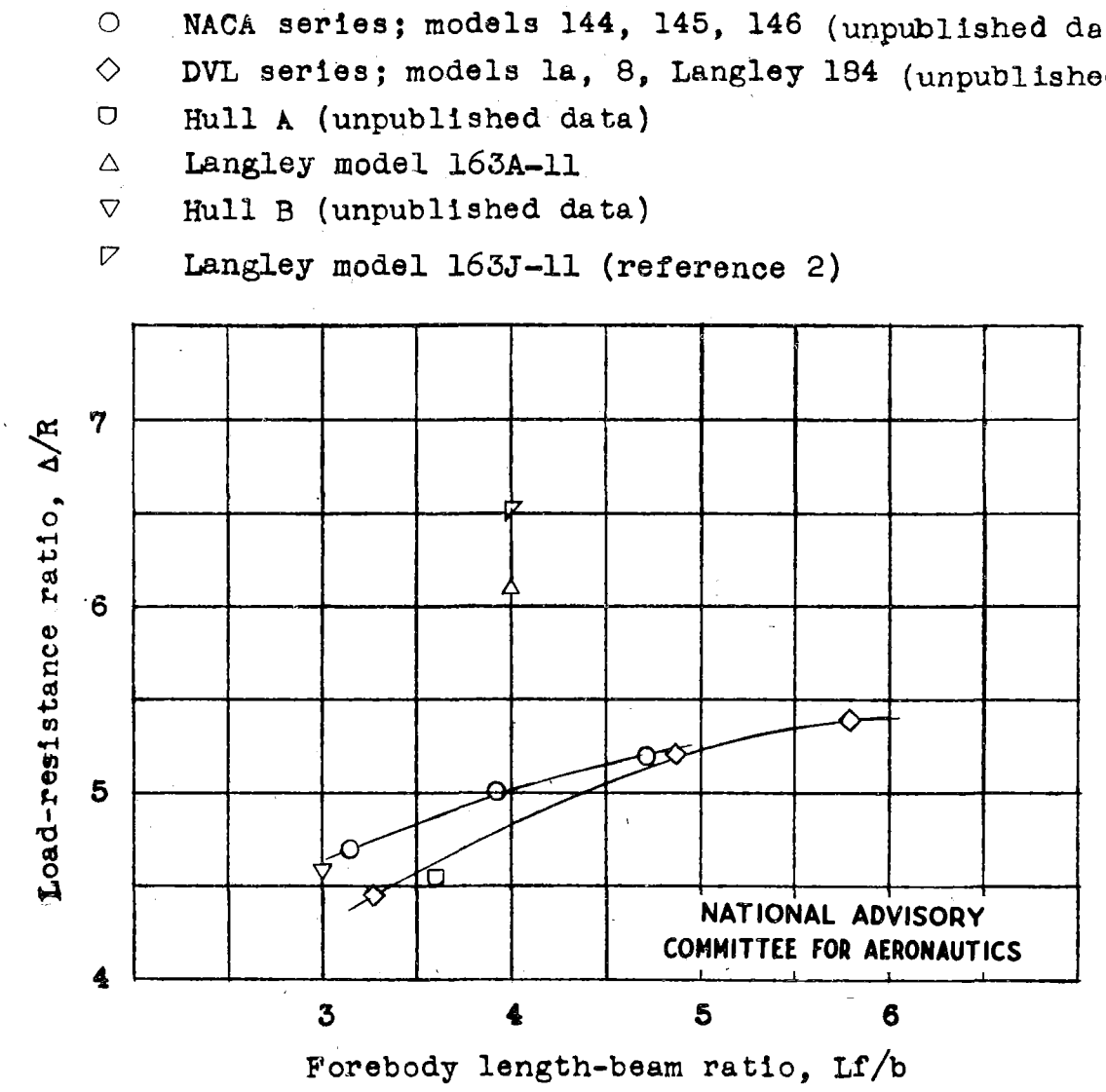

Figure 26.- Effect of forebody length-beam ratio on load-resistance ratio at the hump. $C_{\Delta_o} = 1.00$.

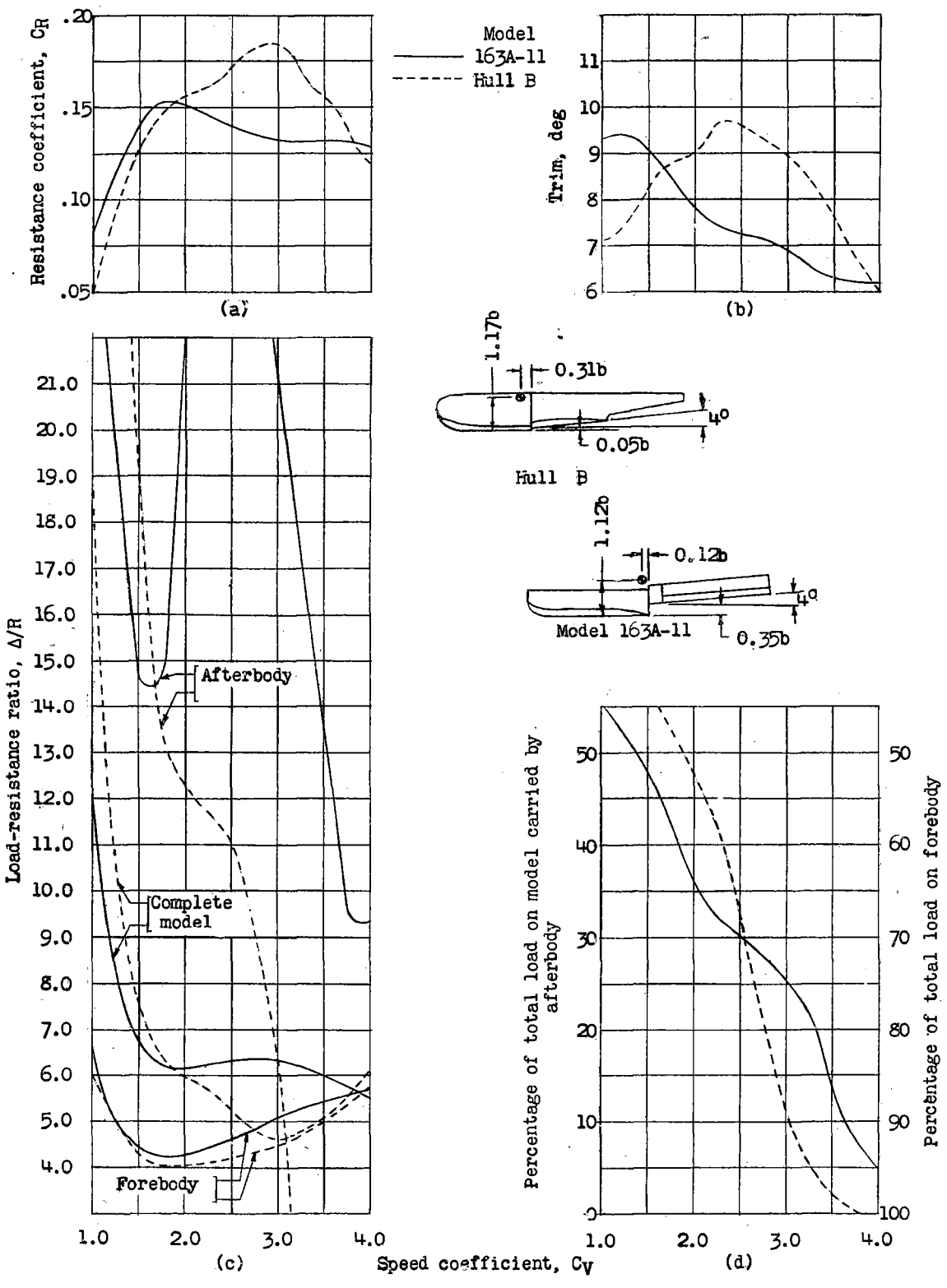

Figure 27.- Comparison of best-trim resistance characteristics of model 163A-11 and hull B. $C_{\Delta_0} = 1.00$.